supershift assays. The results revealed that the NF-κB components consist of p50, p65, and RelB (Fig. 1B).

3.2. DHMEQ induces apoptosis of LCLs

To study the significance of NF-κB activation in the growth of LCLs, we examined the effects of DHMEQ on cell viability. Results of WST-8 assays showed that DHMEQ treatment reduced the cell viability of all four LCLs in a dose- and time-dependent manner (Fig. 2A and B).

NF-κB plays a key role in resistance to apoptosis [18]. Thus, we next examined whether DHMEQ induces apoptosis of LCLs by analyzing Annexin V reactivity and DNA fragmentation. Flow cytometric analysis showed a significant increase in the number of Annexin V-positive cells after DHMEQ treatment (Fig. 3A). Fragmentation of the nuclei of LCLs was clearly demonstrated after DHMEQ treatment by the TUNEL assay (Fig. 3B and C).

3.3. DHMEQ-induced apoptosis involves activation of caspases 3, 8, and 9

To confirm that the induction of apoptosis in LCLs by DHMEQ is caused by activation of the caspase pathway, we first examined activation of caspase-3/7 by immunostaining, using an antibody that recognizes a cleaved form of caspase-3/7. Results clearly showed cleavage of caspase-3/7, confirming that DHMEQ-induced apoptosis is associated with activation of the caspase pathway (Fig. 4A, top). To differentiate the membranous and mitochondrial pathways, we next examined the activation of caspases 8 and 9, which are upstream of caspase-3/7, by immunostaining. DHMEQ-treated LCL cells showed activation of both caspase-8 and caspase-9 (Fig. 4A, middle and bottom).

To understand the molecular mechanisms of apoptosis induction of LCLs after NF-κB inhibition by DHMEQ, we next examined by quantitative RT–PCR the changes in the expression levels of anti-apoptotic genes c-IAP1, Bfl-1, Bcl-XL, and c-FLIP, reportedly under the control of NF-κB, after DHMEQ treatment. The results demonstrated down-regulation of all of these genes (Fig. 4B).

3.4. DHMEQ shows a potent inhibitory effect on the growth of LCL cells in NOG mice

Because results *in vitro* suggested potential efficacy of DHMEQ for the treatment of patients with EBV-associated lymphoproliferative diseases, we next examined whether DHMEQ treatment can suppress the growth of xenografted LCL cells in a NOG mouse model. The gross appearance of resected tumors in mice treated with DHMEQ showed reduction of the tumor mass 1 month after inoculation of LCL cells (Fig. 5A and B). A decrease in the size of tumors in mice treated with DHMEQ was demonstrated when compared with controls 1 month after the injection of LCL cells (Fig. 5C).

3.5. DHMEQ inhibits outgrowth of EBV-infected peripheral blood B-lymphocytes

EBV-infected B lymphocytes under immunocompromised conditions acquire latency III infection, which may lead to proliferation and transformation into lymphoproliferative diseases including lymphomas [2,3]. Previous data link NF-κB activation by LMP-1 to transformation; however, they also indicate that NF-κB activation is not sufficient for transformation and should coordinate with other signals like mitogen-activated protein kinases [19]. Roles of NF-κB activity in EBV-infected lymphocytes for their survival during the early phase of infection are not fully understood. Therefore, to investigate the roles of NF-κB activation on the survival of EBV-infected lymphocytes during the early phase of infection, we examined the effect of NF-κB inhibition by DHMEQ on their survival and the EBV viral load in PBMC infected with EBV. Lymphocytes infected with EBV under immunosuppressive conditions already show constitutive NF-κB activation as well as LMP1 expression. Treatment of these cells with DHMEQ inhibited translocation of NF-κB into the nucleus (Fig. 6A). DHMEQ treatment also eliminated LMP1-expressing lymphocytes from PBMC (Fig. 6B). Finally, DHMEQ treatment prevented the outgrowth of lymphocytes infected

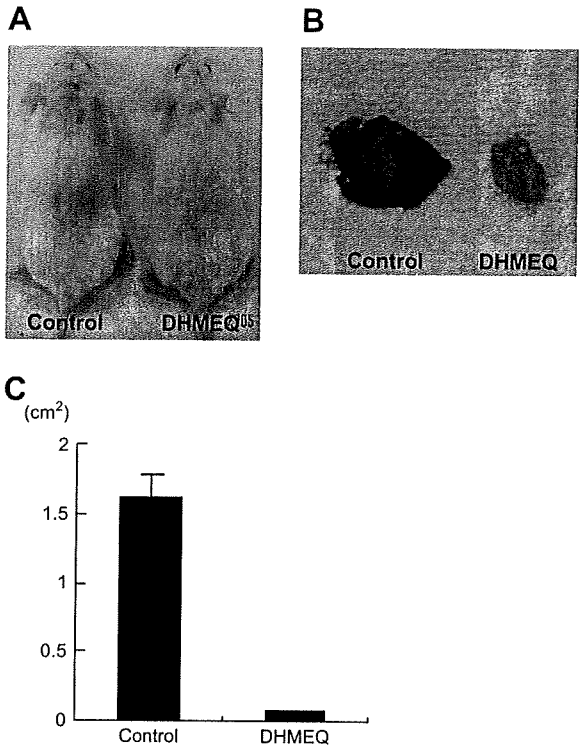

Fig. 5. DHMEQ inhibited the tumor growth of LCL cells *in vivo*. NOG mice were inoculated with LCL cells and administered DHMEQ (12 mg/kg) ($n = 5$) or control medium ($n = 5$) subcutaneously in the post-auricular region three times a week for up to 1 month. (A) Photograph of the backs of mice. (B) Photograph of a tumor at the site of LCL cells inoculation. (C) Subcutaneous tumor volume of mice inoculated with LCL cells and administered DHMEQ or control medium 1 month after inoculation.

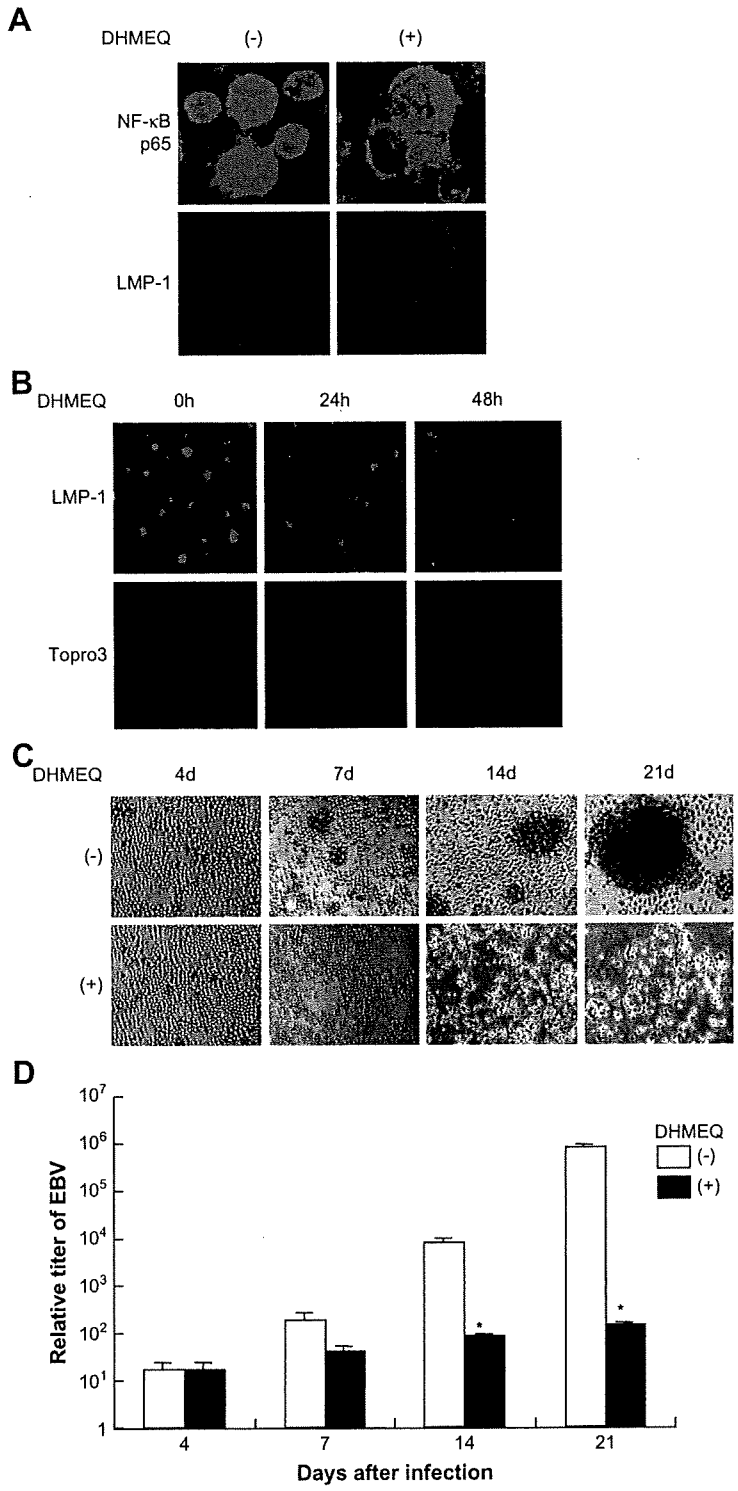

Fig. 6. Effects of DHMEQ on PBMC infected with EBV. 8×10^5/ml of PBMC from a healthy donor infected with EBV using supernatant of B95.8 line were cultured in RPMI 1640 medium supplemented with 10% FBS and 200 ng/ml cyclosporine A. Cells were harvested 4 days and 14 days after infection and served for experiments. (A) Inhibition of NF-κB and expression of LMP1 in lymphocytes. At the point of 4 days after infection, cells were treated with or without 10 μg/ml of DHMEQ for 1 h and immunostained with antibodies for LMP1 and NF-κB p65. DMSO-treated cells served as a control. (B) DHMEQ treatment eliminated LMP1 expressing cells from PBMC. At the point of 14 days after infection, cells were treated with or without 10 μg/ml DHMEQ for the indicated number of hours. Cells stained with anti-LMP1 antibody and topro 3 were observed by confocal microscopy. DMSO-treated cells served as a control. (C, D) Photographs of EBV-infected PBMC and quantification of viral load by real-time PCR. Cells cultured for 4 days were treated with 10 μg/ml of DHMEQ (+) or with DMSO alone (−) thereafter twice a week. Cells were observed by microscopy at the indicated days (C). Cells were harvested on the indicated days and genomic DNA was isolated. The viral load was quantified by real-time PCR as described in Section 2. The data are means and standard deviations of triplicate experiments (D). The asterisks indicate statistical significance.

with EBV and decreased the EBV viral load in PBMC (Fig. 6C and D).

4. Discussion

In the present study, we showed that the NF-κB inhibitor DHMEQ blocked strong and constitutive NF-κB activity, reduced viability, and induced apoptosis in LCLs. Induction of apoptosis by DHMEQ in LCLs is associated with inhibition of NF-κB, which is followed by down-regulation of NF-κB regulated anti-apoptotic genes. These observations, combined with our previous study about the mechanisms of action of DHMEQ [11], indicate that apoptosis induction of LCLs by DHMEQ is mediated by inhibitory effect of DHMEQ against NF-κB. DHMEQ appears to be more specific to NF-κB pathway compared with IκB kinase (IKK) inhibitor, Bay 11-7082 used in the previous studies [20,21], because DHMEQ inhibits downstream of IKK and Bay 11-7082 has been reported to be apparently not specific for NF-κB pathway [22]. Therefore our study provides further evidence for the importance of NF-κB in the survival of LCLs and indicates effectiveness of DHMEQ in the treatment of EBV-infected transformed lymphocytes.

We also showed that DHMEQ inhibits constitutive NF-κB activation in B lymphocytes expressing LMP1, eliminates these cells from PBMC, and inhibits the outgrowth of lymphoblastic cells. The results indicate that B lymphocytes become dependent on NF-κB for proliferation and survival within several days after EBV infection. Although previous data indicate that not only NF-κB but also other signals like mitogen-activated protein kinases are involved in transformation of lymphocytes to LCL cells [19], the results in this study indicates that abrogation of constitutive NF-κB activity appears to be sufficient to prevent transformation of EBV-infected lymphocytes. Previous reports underscored constitutive NF-κB activity as a molecular target in LCL cells [20,21,23]. Our study shows a new insight that constitutive NF-κB activity is a common molecular target in EBV-infected transformed and untransformed lymphocytes.

Recent reports showed that EBV viral load is a useful marker for disease status of lymphoproliferative diseases or lymphomas in patients with immunosuppression [24]. We showed that DHMEQ treatment prevented the increase of EBV viral load in PBMC. The reduction of EBV viral load in PBMC by DHMEQ indicates not only that the elimination of lymphocytes infected by EBV contributes to the reduction, but also that the replication of EBV virus may depend on NF-κB activity. However, previous studies showed that NF-κB activity does not promote replication of EBV virus, but rather inhibits its replication [25]. Therefore, reduction of viral load in lymphocytes infected with EBV treated with DHMEQ appears to be due to the elimination of lymphocytes infected with EBV. Collectively, early detection of the increase of EBV viral load and purging infected cells under transformation by a NF-κB inhibitor may contribute to the preventive intervention against lymphoproliferative diseases in patients with profound immunosuppression.

Our results suggest that the effects of DHMEQ depend on the down-regulation of NF-κB-dependent genes that control apoptosis. Down-regulation of c-FLIP, involved in anti-apoptosis blocking caspase-8, as well as Bfl-1, Bcl-XL and c-IAP, involved in the anti-apoptosis blocking caspase-9, by DHMEQ may result in activation of membranous and mitochondrial pathways, respectively [26]. This implies the possibility that in EBV-infected lymphocytes, the induction of anti-apoptotic genes is counteracting the apoptotic pressure and preventing these cells from undergoing apoptosis.

The mice treated with DHMEQ in 1% DMSO did not show any relevant signs of toxicity such as body weight loss in this experiment. The dose of DHMEQ administered in this experiment was 12 mg/kg three times a week, far less than the LD_{50} of DHMEQ, 180 mg/kg (Naoki Matsumoto, K.U., unpublished observation, July 1999). Results of our in vivo model suggest that DHMEQ may be feasible and less toxic at an effective dose, although the pharmacokinetics has not yet been elucidated. In our NOG mice model, the results indicate that local administration of DHMEQ can prevent primary tumor growth without significant signs of toxicity. Additional experiments, which include intraperitoneal and intravenous administration of DHMEQ, will further confirm efficacy of DHMEQ against LCLs *in vivo*.

Our recent study also indicates that DHMEQ has little effect on the viability of PBMC or purified B cells *in vitro* under almost the same experimental condition as this study [27]. These *in vitro* and *in vivo* results suggest a favorable toxic profile and potent NF-κB inhibitory effect by DHMEQ. Thus, DHMEQ appears to be a candidate for the treatment of EBV-associated lymphoproliferative diseases as well as for their chemoprevention.

In conclusion, our study indicates that the unique NF-κB inhibitor DHMEQ is a potential compound that targets constitutive activation of NF-κB in EBV-infected transformed and untransformed B cells. Because EBV-associated lymphoproliferative diseases are life-threatening and the prognosis of AIDS-associated lymphomas is extremely unfavorable, our results support preventive intervention with a NF-κB inhibitor as a new strategy in patients with immunosuppression.

Acknowledgments

This work was supported in part by Grants-in-Aid for Scientific Research from the Japan Society for Promotion of Science (R.H. and T.W.). This work was also supported by grants from the Japanese Ministries of Education, Culture, Sport Science and Technology and Health, Labour and Welfare, as well as the Human Health Science of Japan (N.Y.).

References

[1] J.I. Cohen, Epstein–Barr virus infection, N. Engl. J. Med 343 (2000) 481–492.
[2] K.F. Macsween, D.H. Crawford, Epstein–Barr virus-recent advances, Lancet Infect. Dis 3 (2003) 131–140.
[3] E. Klein, L.L. Kis, G. Klein, Epstein–Barr virus infection in humans: from harmless to life endangering virus-lymphocyte interactions, Oncogene 26 (2007) 1297–1305.

[4] S. Gottschalk, C.M. Rooney, H.E. Heslop, Post-transplant lymphoproliferative disorders, Annu. Rev. Med 56 (2005) 29–44.
[5] C. Diamond, T.H. Taylor, T. Aboumrad, H. Anton-Culver, Changes in acquired immunodeficiency syndrome-related non-Hodgkin lymphoma in the era of highly active antiretroviral therapy: incidence, presentation, treatment, and survival, Cancer 106 (2006) 128–135.
[6] Y. Hoshida, J.X. Xu, S. Fujita, I. Nakamichi, J. Ikeda, Y. Tomita, S. Nakatsuka, J. Tamaru, A. Iizuka, T. Takeuchi, K. Aozasa, Lymphoproliferative disorders in rheumatoid arthritis: clinicopathological analysis of 76 cases in relation to methotrexate medication, J. Rheumatol 34 (2007) 322–331.
[7] D.C. Guttridge, C. Albanese, J.Y. Reuther, R.G. Pestell, A.S. Baldwin Jr., NF-kappaB controls cell growth and differentiation through transcriptional regulation of cyclin D1, Mol. Cell. Biol. 19 (1999) 5785–5799.
[8] O. Devergne, E. Hatzivassiliou, K.M. Izumi, K.M. Kaye, M.F. Kleijnen, E. Kieff, G. Mosialos, Association of TRAF1, TRAF2, and TRAF3 with an Epstein–Barr virus LMP1 domain important for B-lymphocyte transformation: role in NF-kappaB activation, Mol. Cell. Biol. 16 (1996) 7098–7108.
[9] T.D. Gilmore, Introduction to NF-kappaB: players, pathways, perspectives, Oncogene 25 (2006) 6680–6684.
[10] N. Matsumoto, A. Ariga, S. To-e, H. Nakamura, N. Agata, S. Hirano, J. Inoue, K. Umezawa, Synthesis of NF-kappaB activation inhibitors derived from epoxyquinomicin C, Bioorg. Med. Chem. Lett. 10 (2000) 865–869.
[11] A. Ariga, J. Namekawa, N. Matsumoto, J. Inoue, K. Umezawa, Inhibition of tumor necrosis factor-alpha-induced nuclear translocation and activation of NF-kappa B by dehydroxymethylepoxyquinomicin, J. Biol. Chem. 277 (2002) 24625–24630.
[12] G. Miller, M. Lipman, Comparison of the yield of infectious virus from clones of human and simian lymphoblastoid lines transformed by Epstein–Barr virus, J. Exp. Med 138 (1973) 1398–1412.
[13] N.C. Andrews, D.V. Faller, A rapid micropreparation technique for extraction of DNA-binding proteins from limiting numbers of mammalian cells, Nucleic Acids Res. 19 (1991) 2499.
[14] J. Inoue, L.D. Kerr, L.J. Ransone, E. Bengal, T. Hunter, I.M. Verma, c-rel activates but v-rel suppresses transcription from kappa B sites, Proc. Natl. Acad. Sci. USA 88 (1991) 3715–3719.
[15] M.Z. Dewan, J.N. Uchihara, K. Terashima, M. Honda, T. Sata, M. Ito, N. Fujii, K. Uozumi, K. Tsukasaki, M. Tomonaga, Y. Kubuki, A. Okayama, M. Toi, N. Mori, N. Yamamoto, Efficient intervention of growth and infiltration of primary adult T-cell leukemia cells by an HIV protease inhibitor, ritonavir, Blood 107 (2006) 716–724.
[16] M. Watanabe, M.Z. Dewan, T. Okamura, M. Sasaki, K. Itoh, M. Higashihara, H. Mizoguchi, M. Honda, T. Sata, T. Watanabe, N. Yamamoto, K. Umezawa, R. Horie, A novel NF-kappaB inhibitor DHMEQ selectively targets constitutive NF-kappaB activity and induces apoptosis of multiple myeloma cells in vitro and in vivo, Int. J. Cancer 114 (2005) 32–38.
[17] H. Kimura, M. Morita, Y. Yabuta, K. Kuzushima, K. Kato, S. Kojima, T. Matsuyama, T. Morishima, Quantitative analysis of Epstein–Barr virus load by using a real-time PCR assay, J. Clin. Microbiol. 37 (1999) 132–136.
[18] J. Dutta, Y. Fan, N. Gupta, G. Fan, C. Gelinas, Current insights into the regulation of programmed cell death by NF-kappaB, Oncogene 25 (2006) 6800–6816.
[19] E.D. Cahir McFarland, K.M. Izumi, G. Mosialos, Epstein–Barr virus transformation: involvement of latent membrane protein 1-mediated activation of NF-kappaB, Oncogene 18 (1999) 6959–6964.
[20] E.D. Cahir-McFarland, K. Carter, A. Rosenwald, J.M. Giltnane, S.E. Henrickson, L.M. Staudt, E. Kieff, Role of NF-kappa B in cell survival and transcription of latent membrane protein 1-expressing or Epstein–Barr virus latency III-infected cells, J. Virol 78 (2004) 4108–4119.
[21] S.A. Keller, D. Hernandez-Hopkins, J. Vider, V. Ponomarev, E. Hyjek, E.J. Schattner, E. Cesarman, NF-kappaB is essential for the progression of KSHV- and EBV-infected lymphomas in vivo, Blood 107 (2006) 3295–3302.
[22] J.W. Pierce, R. Schoenleber, G. Jesmok, J. Best, S.A. Moore, T. Collins, M.E. Gerritsen, Novel inhibitors of cytokine-induced IkappaBalpha phosphorylation and endothelial cell adhesion molecule expression show anti-inflammatory effects in vivo, J. Biol. Chem. 272 (1997) 21096–21103.
[23] E.D. Cahir-McFarland, D.M. Davidson, S.L. Schauer, J. Duong, E. Kieff, NF-kappa B inhibition causes spontaneous apoptosis in Epstein–Barr virus-transformed lymphoblastoid cells, Proc. Natl. Acad. Sci. USA 97 (2000) 6055–6060.
[24] S.M. Aalto, E. Juvonen, J. Tarkkanen, L. Volin, T. Ruutu, P.S. Mattila, H. Piiparinen, S. Knuutila, K. Hedman, Lymphoproliferative disease after allogeneic stem cell transplantation–pre-emptive diagnosis by quantification of Epstein–Barr virus DNA in serum, J. Clin. Virol 28 (2003) 275–283.
[25] H.J. Brown, M.J. Song, H. Deng, T.T. Wu, G. Cheng, R. Sun, NF-kappaB inhibits gammaherpesvirus lytic replication, J. Virol 77 (2003) 8532–8540.
[26] J.M. Adams, Ways of dying: multiple pathways to apoptosis, In: Genes Dev, 17 (2003) 2481–2495.
[27] R. Horie, M. Watanabe, T. Okamura, M. Taira, M. Shoda, T. Motoji, A. Utsunomiya, T. Watanabe, M. Higashihara, K. Umezawa, DHMEQ, a new NF-kappaB inhibitor, induces apoptosis and enhances fludarabine effects on chronic lymphocytic leukemia cells, Leukemia 20 (2006) 800–806.

ELSEVIER

INSTITUT PASTEUR

Microbes and Infection 10 (2008) 471–480

www.elsevier.com/locate/micinf

Original article

Statin-induced inhibition of HIV-1 release from latently infected U1 cells reveals a critical role for protein prenylation in HIV-1 replication

Tohti Amet [a], Mizuho Nonaka [a], Md. Zahidunnabi Dewan [a,b], Yasunori Saitoh [a], Xiaohua Qi [a,b], Shizuko Ichinose [c], Naoki Yamamoto [a,b], Shoji Yamaoka [a,*]

[a] *Department of Molecular Virology, Graduate School of Medicine, Tokyo Medical and Dental University, 1-5-45 Yushima, Bunkyo-ku, Tokyo 113-8510, Japan*

[b] *AIDS Research Center, National Institute of Infectious Diseases, Shinjuku-ku, Tokyo 162-8640, Japan*

[c] *Instrumental Analysis Research Center, Tokyo Medical and Dental University, 1-5-45 Yushima, Bunkyo-ku, Tokyo 113-8510, Japan*

Received 20 November 2007; accepted 14 January 2008
Available online 20 January 2008

Abstract

Latent infection of human immunodeficiency virus type 1 (HIV-1) represents a major hurdle in the treatment of acquired immunodeficiency syndrome (AIDS) patients. Statins were recently reported to suppress acute HIV-1 infection and reduce infectious virion production, but the precise mechanism of inhibition has remained elusive. Here we demonstrate that lypophilic statins suppress HIV-1 virion release from tumor necrosis factor alpha-stimulated latently infected U1 cells through inhibition of protein geranylgeranylation, but not by cholesterol depletion. Indeed, this suppression was reversed by the addition of geranylgeranylpyrophosphate, and a geranylgeranyltransferase-1 inhibitor reduced HIV-1 production. Notably, silencing of the endogenous Rab11a GTPase expression in U1 cells by RNA interference destabilized Gag and reduced virion production both in vitro and in NOD/SCID/γc^{null} mice. Our findings thus suggest that small GTPase proteins play an important role in HIV-1 replication, and therefore could be attractive molecular targets for anti-HIV-1 therapy.

Keywords: Statins; Prenylation; HIV-1; Rab11a; Small GTPases

1. Introduction

Infection with human immunodeficiency virus type 1 (HIV-1), the causative agent of acquired immunodeficiency syndrome (AIDS), is characterized clinically by a long asymptomatic period of latency preceding the development of AIDS. Even during this period of latency, the virus is continuously replicating and causing *de novo* infection. Recent studies using combination anti-retroviral therapy have revealed a population of latently infected cells that are refractory to antiviral therapy, which is believed to be a leading cause of the persistence of infection [1]. Although patients treated successfully with the highly active anti-retroviral therapy (HAART) achieved undetectable levels of virus load, viremia recurred in almost every patient when the drug therapy was stopped, because latent virus in reservoir cells is not susceptible to this anti-retroviral therapy or host immune responses [2,3]. Thus, HIV-1 infection remains incurable and new therapeutic approaches need to be developed.

Recent studies have suggested that lypophilic statins have direct anti-HIV effects. del Real et al. showed that lovastatin reduced acute infection by HIV-1 NL4-3.Luc.R.E. pseudotyped with HIV-R5 or X4 envelopes, but not that by the virus pseudotyped with the vesicular stomatitis virus glycoprotein (VSV-G) envelope. Lovastatin treatment of HEK 293T producer cells also reduced HIV-1-X4-enveloped infectious virus production, but not that of VSV-G-pseudotyped virus. The

* Corresponding author. Tel.: +81 3 5803 5181; fax: +81 3 5803 0124.
E-mail address: shojmmb@tmd.ac.jp (S. Yamaoka).

1286-4579/$ - see front matter © 2008 Elsevier Masson SAS. All rights reserved.
doi:10.1016/j.micinf.2008.01.009

proposed mechanism was that statins targeted Rho GTPases and affected the actin cytoskeleton re-arrangement necessary for virus entry or budding [4,5]. It was also reported that statins suppressed virion-associated intercellular cell adhesion molecule 1–leukocyte function antigen 1 interactions that are required for viral entry [6]. Audoly et al., using inhibitory toxins, proposed that small GTP-binding proteins are involved in the assembly of HIV-1 Gag in their acute infection model [7]. Quite recently, Nabatov et al. reported that statins disrupt CCR5 and RANTES expression levels in CD4+ T lymphocytes in vitro and preferentially decrease infection of R5 versus X4 HIV-1 [8]. However, the effect of statins in chronically HIV-1-infected cells and its precise mechanism remain to be uncovered.

Statins, which are used to treat hypercholesterolemia, inhibit 3-hydroxy-3-methylglutaryl coenzyme A (HMG-CoA) reductase, the rate-limiting enzyme in cholesterol biosynthesis in the liver catalyzing the conversion of HMG-CoA to mevalonic acid [9,10]. In addition to inhibiting cholesterol synthesis, statins also block the synthesis of isoprenoid intermediates such as farnesylpyrophosphate (FPP) and geranylgeranylpyrophosphate (GGpp). Both FPP and GGpp serve as important lipid attachments for the post-translational modification of variety of proteins, including heterotrimeric G proteins and small GTP-binding proteins such as the Ras, Rho, Rap, and Rab GTPase family proteins [11,12]. This modification, called protein prenylation, is a common mechanism for membrane association of approximately 0.5% of all intracellular proteins. Prenylation consists of the covalent attachment, via thioether linkage, of a C15 (farnesyl) or C20 (geranylgeranyl) isoprenoid group to a C-terminal cysteine residue in the context of a 'prenylation motif'. Farnesyl and geranylgeranyl moieties can bind covalently to several low molecular weight GTPase proteins, and this binding is catalyzed by three prenyltransferases: farnesyltransferase (FTase), geranylgeranyltransferase-1 (GGTase-I) or geranylgeranyltransferase-2 (GGTase-2, also called Rab GGTase). Thus, inhibition of the mevalonate pathway or geranylgeranyltransferases leads to impairment of protein prenylation.

Protein prenylation is critical for intracellular localization and function of small GTPase proteins. In general, modification with FPP is necessary for proper localization of Ras family proteins, whereas GGpp is required for Rho, Rab, and Rap family proteins. Among them, Rab GTPase proteins form the largest family within the Ras-like GTPase superfamily [13,14]. More than 50 Rab proteins have been identified in mammalian cells. Each Rab is believed to be localized to a specific subcellular compartment, reflecting the complexity and variety of trafficking events found in mammalian cells. Rab proteins, unlike other small GTPases, exhibit a variety of prenylation motifs at their C-termini, containing either one or more frequently, two cysteine residues, both of which are modified by geranylgeranyl groups [15]. It was recently reported that siRNA-mediated silencing of Rab9 expression in JC53 HeLa-derived indicator cells inhibited HIV replication, as did silencing expression of other genes that facilitate the late-endosome-to-*trans*-Golgi vesicular transport [16]. Interestingly, acute HIV-1 replication in JC53 cells was also affected, although less profoundly, by silencing expression of Rab11a. It has been well documented that Rab11a is mainly located on pericentriolar recycling endosomes and plays a key role in regulating vesicle trafficking through recycling endosomes to the plasma membrane as well as in exocytosis [17,18].

Here we investigated the effect of statins on virus production in chronically HIV-1-infected promonocytic U1 cells, and showed a critical role for protein prenylation in the late phase of HIV-1 replication.

2. Materials and methods

2.1. Reagents and cells

Simvastatin and lovastatin were purchased from LKT Laboratories, Inc. (MN, USA), and activated by dissolving in ethanol and treatment with 0.1 M NaOH. The pH was then adjusted to 7.0 with HCl. GGTI-298 and FTI-277 were purchased from Calbiochem (Darmstadt, Germany). Anti-Rab11a monoclonal antibody was purchased from BD transduction laboratories (Japan). The serum derived from an HIV-1-infected patient was described previously [19]. Anti-mouse IgG (H&L), anti-human rabbit HRP-linked antibody was obtained from American Qualex manufactures (CA, USA). DMRIE-C reagent for transfection was purchased from Invitrogen (CA, USA). All other reagents including anti-tubulin (T-9026) monoclonal antibody, squalene, GGpp, cycloheximide, TNF-α and phorbol-12-myristate-13 acetate (PMA) were purchased from Sigma (MO, USA). U1 and HEK 293T cells were grown in RPMI 1640 and DMEM, respectively, supplemented with 10% heat-inactivated fetal bovine serum, 100 U/ml of penicillin and streptomycin at 37 °C.

2.2. Treatment and stimulation of cells

Cells were treated with or without simvastatin or lovastatin for 2 days and equivalent numbers of viable cells were stimulated with TNF-α or PMA for additional 2 days in the presence or absence of statins, and then intracellular and extracellular Gag (p24 and p55) antigen was quantified. More than 80% of cells were found viable after treatment with 1 μM of simvastatin, and we normalized the levels of Gag protein (p24 and p55) based on the number of viable cells in each sample. The amount of Gag per viable cell was calculated by dividing the Gag value with the number of viable cells. In some of the experiments, GGpp (1 μM), squalene (50 μg/ml) or GGTI-298 (1 μM) was added during the entire course of the experiment.

2.3. HIV-1 Gag quantification

Culture supernatant was collected after centrifugation and subjected to quantification of the HIV-1 Gag (p55 and p24) antigen by automated enzyme-linked immunosorbent assay (ELISA) (Fuji Rebio Inc., Tokyo, Japan). Cell pellets were

washed three times with PBS, re-suspended with the p24 lysis buffer (0.5% Triton X-100 in PBS), put on ice for 30 min, and then the Gag antigen was quantified by using auto-ELISA system. The amount of Gag was normalized by dividing the Gag value with the number of viable cells. The relative amounts of Gag were expressed as percentages of that for cells simply stimulated with TNF-α or PMA (arbitrarily set at 100%). The ratio of Gag amount in culture supernatant to that in cells was calculated by dividing the normalized Gag amount in supernatant with that in cell lysate.

2.4. Western blotting

Cells were lysed in a lysis buffer (20 mM Tris–HCl [pH 8.0], 150 mM NaCl, 1% Triton X-100, 10% glycerol, 0.5 mM dithiothreitol, 0.5 mM phenylmethanesulphonylfluoride (PMSF), 0.1% aprotinin, and 0.1% leupeptin) for preparation of whole-cell extracts. Thirty micrograms aliquots of protein, determined by the Bradford assay, were resolved by SDS–PAGE and detected by standard immunoblotting procedures using the specific primary antibodies.

2.5. Transmission electron microscopy

Cells were fixed with 2.5% glutaraldehyde in PBS for 2 h, washed and fixed overnight at 4 °C in the same buffer and post-fixed with 1% OsO_4 buffered with PBS for 2 h. The cells were then dehydrated in a graded series of ethanol and embedded in Epon 812. Ultrathin (90 nm) sections were cut on an ultracut S microtome (Reichert, Vienna, Austria), double-stained with uranyl acetate and lead citrate, and then examined by transmission electron microscopy (H-7100, Hitachi, Hitachinaka, Japan).

2.6. Lentivirus vectors

Annealed oligonucleotides containing the targeting *rab11a* (5′-GAGCGATATCGAGCTATAA-3′) or *Renilla luciferase* (5′-GTAGCGCGGTGTATTATAC-3′) sequence were first inserted immediately downstream of the H1 promoter of the pSuperRetro vector (Oligoengine), generating pSR-Rab11a-i and pSR-Ctrl-i, respectively. The shRNA expression cassettes were then transferred to a newly constructed lentivirus vector, pCS-puro-PRE, carrying a puromycin resistance gene expressed under the control of the phosphoglycerate kinase (PGK) promoter. Construction details for pCS-puro-PRE will be described elsewhere (Saitoh et al., unpublished). EcoRI–XhoI fragments containing the H1 promoter and targeting sequence from pSR-Rab11a-i or pSR-Ctrl-i were inserted between the EcoRI and XhoI sites of pCS-puro-PRE, generating pCS-puro-Rab11a-i and pCS-puro-Ctrl-i, respectively.

2.7. Transfection and infection

The VSV-G-pseudotyped lentivirus was produced by co-transfection of HEK 293T cells with pCS-puro-Rab11a-i or pCS-puro-Ctrl-i, pHCMV-VSV-G encoding the vesicular stomatitis virus glycoprotein (VSV-G) and a packaging construct pCMVΔR8.2 (a kind gift from ISY Chen, USA), using FuGENE 6 (Roche Diagnostics, IN, USA) according to the manufacturer's instructions. Culture supernatants of 293T cells were collected 48 h post-transfection, filtered through 0.20-μm pore-size filters, supplemented with polybrene (10 μg/ml), and used immediately for infection of U1 cells. Infected cells were selected in the presence of 3 μg/ml of puromycin.

2.8. Animal experiments

NOD/SCID/γc^{null} (NOG) mice were obtained from the Central Institute for Experimental Animals (Kawasaki, Japan). All mice were maintained under specific pathogen-free conditions in the animal center of Tokyo Medical and Dental University (Tokyo, Japan). The Ethical Review Committee of the Institute approved the experimental protocol. NOG mice were inoculated intraperitoneally with approximately 2.5×10^6 Rab11a-depleted or control U1 cells per mouse as described previously [20]. Blood and ascites were examined for HIV-1 p24 amount 2 weeks after cell inoculation.

3. Results

3.1. Statins suppressed HIV-1 release from U1 cells

We used U1 cells that do not constitutively produce or release HIV-1 virions to the culture supernatant. U1 cells are derived from U937 promonocytic cells that survived the cytopathic effect associated with the acute infection by HIV-1 LAI/IIIB. U1 cells contain two integrated copies of proviral HIV-1 DNA and are characterized by low constitutive levels of virus expression that can be up-regulated by several cytokines and phorbol esters. Upon stimulation of U1 cells with PMA or with cytokines such as TNF-α, a dramatic increase in HIV-1 gene expression and robust virion release can be induced. Virions were shown to be released from U1 cells in a manner similar to that for cells of monocytic lineage [21,22]. U1 cells were treated with or without simvastatin for 48 h and then stimulated with TNF-α. We found that treatment of U1 cells with 1 μM of simvastatin, which is within the clinically relevant range, suppressed TNF-α-induced release of p24 to culture supernatant (Fig. 1A). Conversely, intracellular Gag protein (including both p55 and its processed form p24) was increased after the treatment with simvastatin and TNF-α. As a result, the ratio of Gag in culture supernatant to Gag in cell lysate was reduced (Fig. 1B). The release of p24 from cells treated with simvastatin and PMA (Fig. 1A,B) was not profoundly suppressed, but this treatment increased intracellular level of Gag. Essentially similar results were obtained with another lipophilic statin lovastatin (Fig. 1C,D), but not with hydrophilic paravastatin (data not shown), suggesting that lypophilic statins, such as simvastatin and lovastatin, successfully entered cultured cells and worked as HMG-CoA reductase inhibitors.

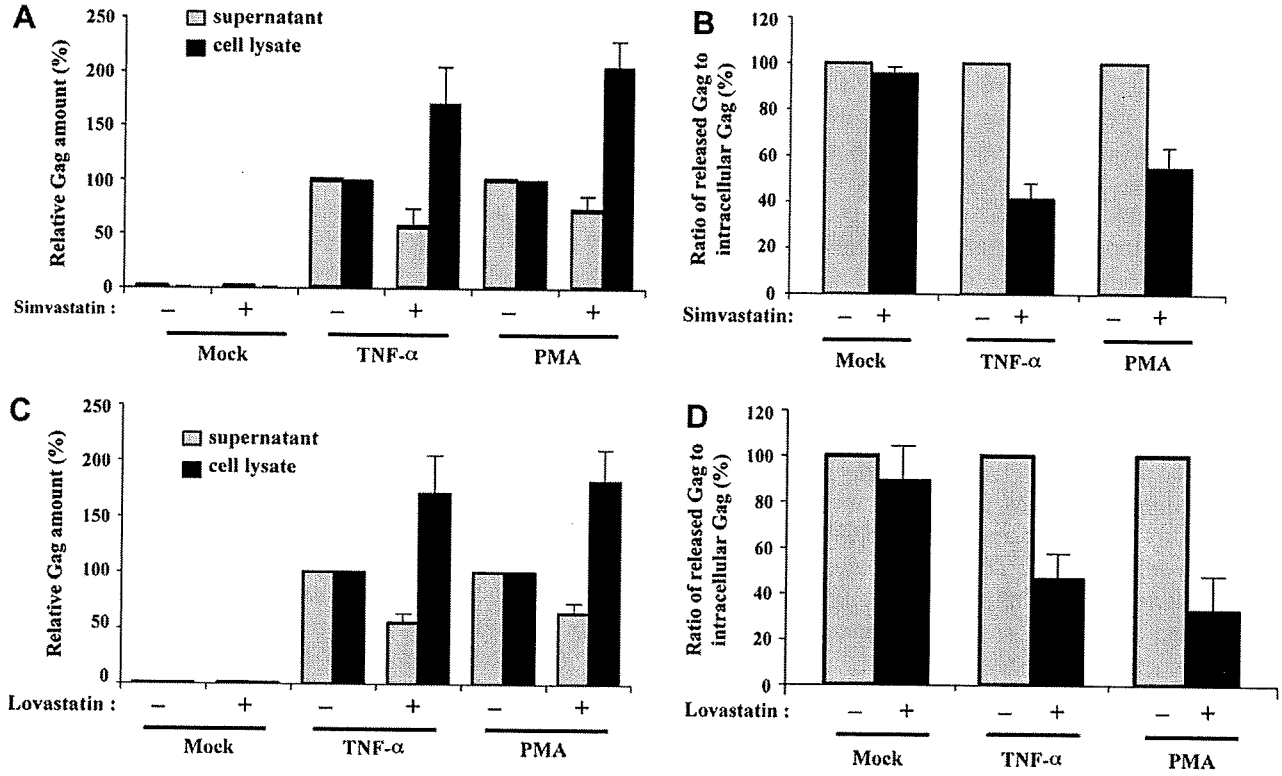

Fig. 1. Statins reduced virus release and increased intracellular Gag in U1 cells. U1 cells were treated or not with simvastatin (A) or lovastatin (C) for 2 days, followed by stimulation with TNF-α (1 ng/ml) or PMA (1 ng/ml) for additional 2 days in the continued presence or absence of simvastatin or lovastatin. Gag (p24 and p55) in culture supernatants (gray bars) and in cell lysates (filled bars) were then quantified. (A) and (C) The relative amounts of Gag in statin-treated (+) cultures are shown in percentage of that of cells (−) stimulated with TNF-α or PMA alone (arbitrarily set at 100%). (B) and (D) Ratios of released Gag to intracellular Gag for statin-treated cells are shown in percentage of the ratio obtained for cells simply stimulated with TNF-α or PMA (arbitrarily set at 100%). Results shown are mean ± SD values of three independent experiments.

3.2. Geranylgeranylation is required for HIV-1 replication in U1 cells

A previous report showed that treatment of 293T cells with lovastatin reduced production of wild type, but not VSV-G-pseudotyped HIV-1, and that this inhibition was reversed by the addition of GGpp [4]. To examine if the reduced p24 release from U1 cells treated with simvastatin resulted from impaired production of geranylgeranyl, we treated U1 cells with simvastatin and TNF-α in the presence of 1 μM GGpp (Fig. 2A). No cytotoxicity was observed after the treatment with GGpp. Addition of GGpp restored the p24 release to the level for control cells stimulated with TNF-α. In contrast, the amount of Gag in cells treated with simvastatin and TNF-α in the presence of GGpp remained higher than that in cells treated with simvastatin and TNF-α. Squalene, one of the metabolites in the cholesterol biosynthesis from FPP, did not interfere with simvastatin-induced inhibition of virion release or intracellular Gag protein accumulation (Fig. 2B). To further investigate the importance of protein prenylation in HIV-1 replication in U1 cells, we tested if geranylgeranyltransferase-1 inhibitor (GGTI) could inhibit virus replication. GGTI was not toxic to U1 cells at 1 μM, whereas farnesyltransferase inhibitor (FTI) was too toxic to be tested in U1 cells (data not shown). GGTI reduced both p24 release and intracellular Gag in TNF-α-stimulated U1 cells (Fig. 2C), suggesting that geranylgeranylation of small GTPase proteins plays a critical role in HIV-1 production.

3.3. Simvastatin enhances intracellular Gag accumulation in U1 cells

We next examined how simvastatin modifies expression of intracellular HIV-1 Gag-related proteins, p55 and its processed form p24. Immunoblotting with anti-HIV-1 Gag antiserum that detected both p55 and p24 revealed that p24 was increased in the presence of simvastatin, while the amount of p55 remained almost unchanged (Fig. 3A). Since the results shown in Fig. 2A suggested the importance of geranylgeranylation, we examined the prenylation status of Rab11a, one of the Rab family small GTPases known to be involved in trafficking of recycling endosomes and exocytosis. As shown in Fig. 3A, treatment with 1 μM simvastatin resulted in almost complete upward shifting of the Rab11a band, indicating accumulation of the non-prenylated form of Rab11a. Besides, GGpp counteracted the simvastatin effect on the prenylation of Rab11a (Fig. 3B). This suggests that simvastatin inhibited the biosynthesis of geranylgeranyl, leading to impaired prenylation of small GTPases involved in intracellular vesicle trafficking. To further gain insight into the effects of simvastatin on HIV-1 replication, we performed transmission electron microscopic (TEM) analysis. Many virus particles were found to be

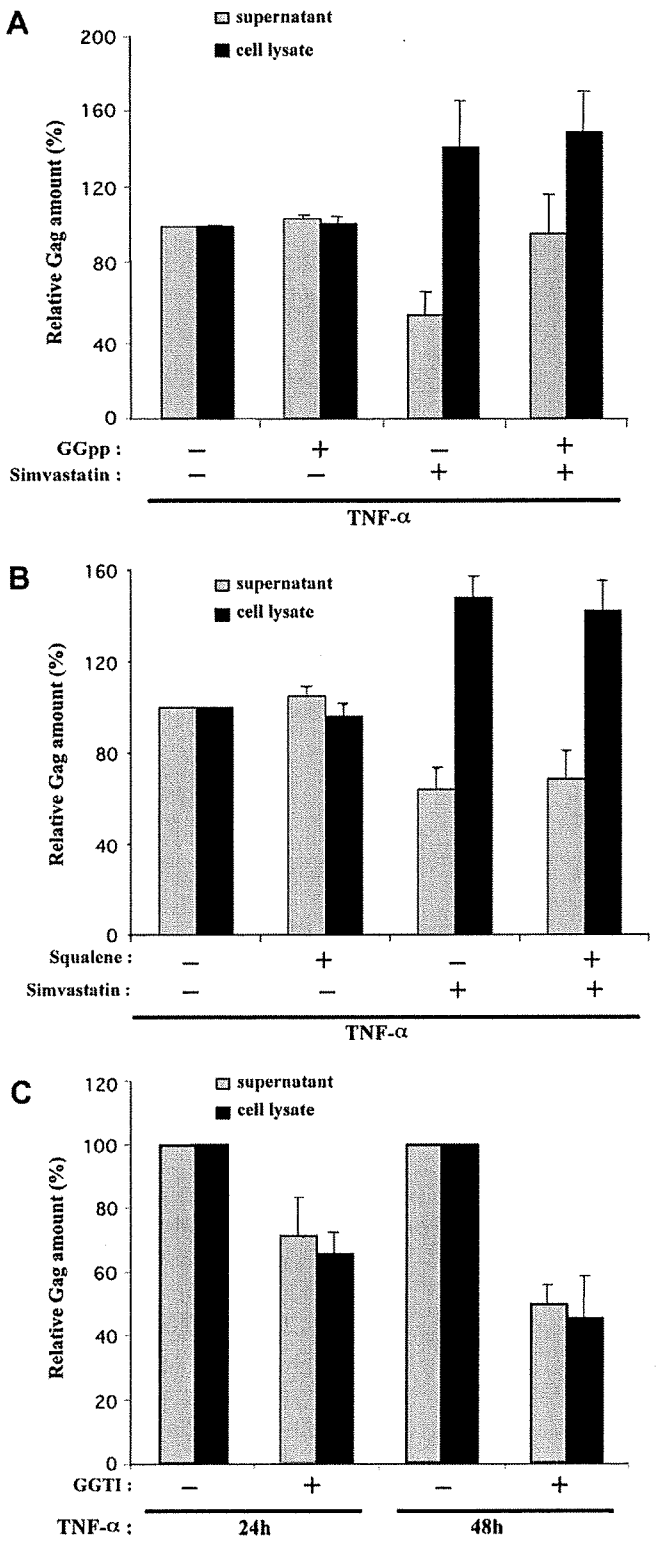

Fig. 2. GGpp restored simvastatin-inhibited virion release, and GGTI suppressed HIV-1 Gag production in U1 cells. U1 cells were cultured for 2 days in the presence (+) or absence (−) of simvastatin, GGpp (A), squalene (B), and GGTI (C). Cells were then stimulated with TNF-α (1 ng/ml) for additional 1 or 2 days, and Gag in supernatants (hatched bars) and cell lysates (filled bars) was quantified. The relative amounts of Gag are shown in percentage of that of cells simply stimulated with TNF-α (arbitrarily set at 100%). Data shown are mean ± SD values of three independent experiments.

released from TNF-α-stimulated U1 cells in the mature form (Fig. 4A,B), but only a few from simvastatin- and TNF-α-treated U1 cells. In contrast, many mature virus particles could be seen in intracellular vesicles of U1 cells treated with simvastatin and TNF-α, whereas it was difficult to find mature virions in vesicles of U1 cells treated with TNF-α alone (Fig. 4C,D). These results suggested impaired release or intracellular trafficking of virions.

3.4. Rab11a mediates HIV-1 replication in U1 cells

In order to further investigate the role of Rab11a in HIV-1 replication in U1 cells, we suppressed the expression of endogenous Rab11a by RNA interference. Immunoblotting analyses (Fig. 5A) demonstrated that the level of Rab11a expression was reduced by ~80–90% in cells expressing Rab11a-specific shRNA (Rab11a-i) compared to cells expressing control shRNA (Ctrl-i). While Rab11a depletion did not affect the growth of U1 cells (data not shown), it reduced the release of p24 as well as intracellular Gag expression induced by TNF-α (Fig. 5B). Immunoblotting analyses revealed that both p24 Gag and p55 Gag are decreased in Rab11a-depleted cells compared to control cells (Fig. 5C). These findings indicate that HIV-1 requires Rab11a for its efficient replication in U1 cells. We next examined if Rab11a depletion affects the stability of Gag, using a protein synthesis inhibitor cycloheximide. As shown in Fig. 5C, the levels of p55 Gag and p24 Gag in Rab11a-depleted cells were generally lower than those in control cells. Importantly, while the expression of p55 Gag remained almost unchanged up to 12 h after CHX treatment in control cells, p55 Gag in Rab11a-depleted cells rapidly decreased with a half-life of ~6 h (Fig. 5D,E). The expression of p24 Gag in Rab11a-depleted cells was lost even more rapidly following cycloheximide treatment, while p24 Gag was only marginally reduced in control cells. These results indicate that Rab11a depletion reduced the stability of Gag, which led to inefficient viral replication in U1 cells.

3.5. Rab11a depletion affects HIV-1 replication in NOG mice

The significant suppression by Rab11a depletion of TNF-α-induced HIV-1 replication in cultured U1 cells prompted us to examine whether depletion of Rab11a in U1 cells can also suppress virus replication in NOG mice. We inoculated Rab11a-depleted or control U1 cells in the peritoneal cavity of immune-deficient NOG mice. Blood and ascites were recovered 2 weeks after inoculation, and then the Gag amounts were determined. Knockdown of Rab11a expression in U1 cells did not apparently influence the growth of cells in mice, but efficiently suppressed HIV-1 replication *in vivo* as revealed by Gag amounts in both serum and ascites (Fig. 6A,B).

4. Discussion

The inhibition of HIV-1 replication by statins was previously reported in acute HIV-1 infection models, and three

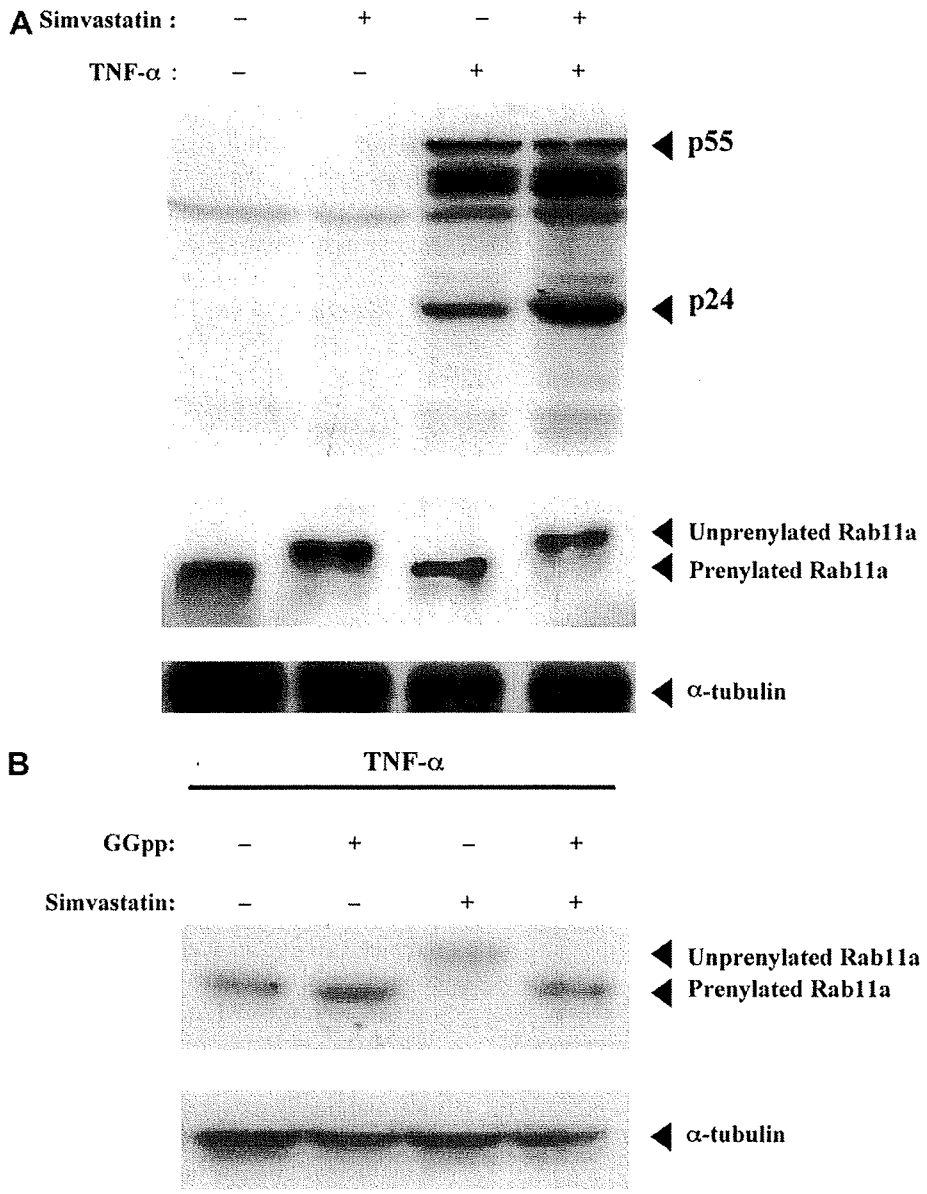

Fig. 3. Simvastatin increased p24 and ablated prenylation of Rab11a in U1 cells. U1 cells were incubated for 2 days with or without simvastatin (A) or GGpp (B), and then stimulated with TNF-α in the continued presence or absence of simvastatin or GGpp for additional 2 days. Whole-cell lysates were prepared and subjected to immunoblotting with serum derived from an HIV-1-infected patient or antibodies to Rab11a or α-tubulin.

different mechanisms were proposed. First, inhibition of HMG-CoA reductase activity resulted in impaired synthesis of GGpp required for prenylation of a small GTPase protein Rho [4]. Second, direct binding of statins to lymphocyte-function-associated antigen 1 (LFA-1) diminished HIV-1 attachment to target cells by preventing the interaction between virion-associated host intercellular adhesion molecule 1 and its natural cell surface ligand LFA-1 [6]. Third, statins disrupted CCR5 and RANTES expression [8]. In this report, we showed statin-induced increase in intracellular Gag and decrease in virus release from chronically HIV-1 infected cells, and defined diminished geranylgeranylation as a principal mechanism of statin-induced inhibition of virus release. The inhibition was associated with nearly a complete loss of prenylation of a small GTPase protein Rab11a, which facilitates vesicle trafficking to the plasma membrane from both the *trans*-Golgi network and recycling endosomes. Indeed, RNA interference-mediated silencing of Rab11a expression also led to a marked reduction in both intracellular and secreted Gag protein. These observations are not limited to TNF-α-induced HIV-1 production in vitro, because the silencing of Rab11a expression also reduced p24 release from U1 cells inoculated in immune-deficient mice.

The effects of simvastatin on HIV-1 replication in U1 cells, increase in intracellular Gag and decrease in virus release, cannot solely be explained by the loss of functional small GTPases involved in vesicle trafficking, because supplementing GGpp in the presence of simvastatin, indeed, restored virus release, but did not normalize the level of intracellular Gag. The increase in intracellular Gag by simvastatin treatment

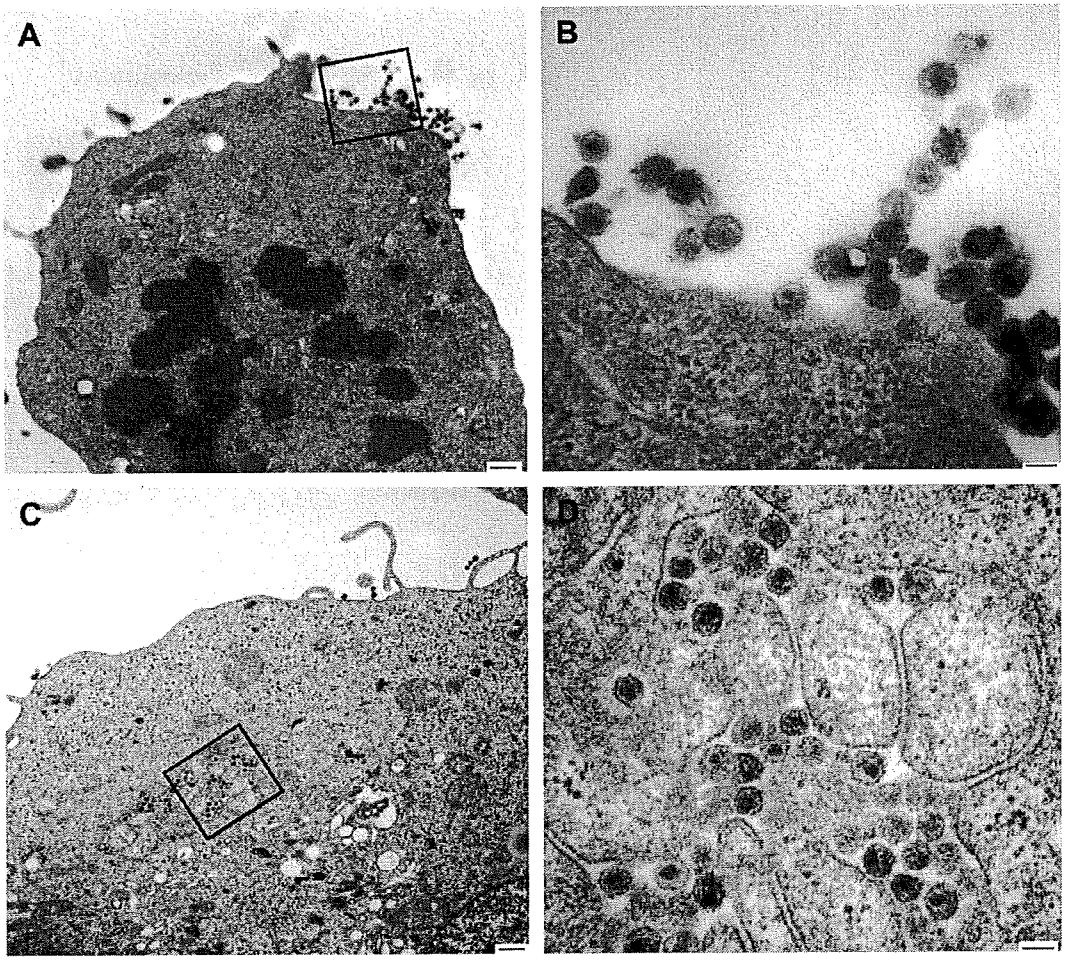

Fig. 4. Transmission electron microscopic (TEM) images of U1 cells. (A) TNF-α-stimulated U1 cell. Many HIV-1 particles are visible at the cell surface. Bar indicates 500 nm (10,000×). (B) Higher magnification of the area indicated by the square in (A). The cone-shaped core structure is evident. Bar indicates 100 nm (60,000×). (C) U1 cell treated with simvastatin and TNF-α. Large vesicles near the Golgi zone contain maturated HIV-1 particles. Bar indicates 500 nm (10,000×). (D) Higher magnification of the area indicated by the square in (C). Bar indicates 100 nm (60,000×).

might simply be a result of accumulation of virions due to impaired virion release, but the results of more specified inhibition by GGTI or gene silencing indicate that loss of prenylation or depletion of Rab11a GTPase reduces both intracellular and extracellular Gag. Thus, simvastatin appears to have yet unknown actions to increase intracellular p24 in U1 cells. In this regard, simvastatin may potentially enhance production of Gag as lovastatin was previously reported to augment HIV-1 LTR-directed transcription in Jurkat cells [4]. The inhibition of virus release by simvastatin would, therefore, be due to loss of prenylation of a yet unidentified protein.

Recent reports support a model of intracellular Gag trafficking common to a variety of cell types in which Gag localizes initially to perinuclear clusters, and then to late endosomes and MVBs and/or MVB-like compartments [23,24]. Both in macrophages and dendritic cells, HIV-1 Gag can be detected in CD63-positive late endosomes and viral exit proceeds through TSG101-dependent budding into the lumen of late endosomes to form multivesicular bodies, followed by the export of viral particles as exosomes [25–28]. However, the transport mechanism of endosomal compartments or MVBs to the cell surface during the course of viral maturation and budding remains to be fully elucidated. Small GTPase proteins have been reported to be involved in vesicle trafficking and actin polymerization. It should be noted that Rab11a is mainly located on pericentriolar recycling endosomes and regulates vesicle trafficking through recycling endosomes to the plasma membrane as well as release of exosomes [29]. In the present report, depletion of Rab11a resulted in an obvious destabilization of Gag p55 and p24, suggesting that Gag failed to traffic through the endosomal compartments or MVBs and could be directed to lysosomal degradation.

Since lipophylic statins cannot be used for HIV-1 infected patients due to its pharmacokinetic interaction with protease inhibitors, inhibiting prenylation of small GTPases involved in Gag trafficking by GGTIs could represent an alternative strategy for effective anti-HIV-1 therapy. GGTI used in this study was previously reported to arrest human tumor cells in G0/G1 and induces $p21^{WAF1/CIP1/SDI1}$ expression in a p53-independent manner and was considered potentially useful in cancer therapy [30]. Perhaps, specific inhibition of individual GTPases involved in HIV-1 replication such as Rab11a would

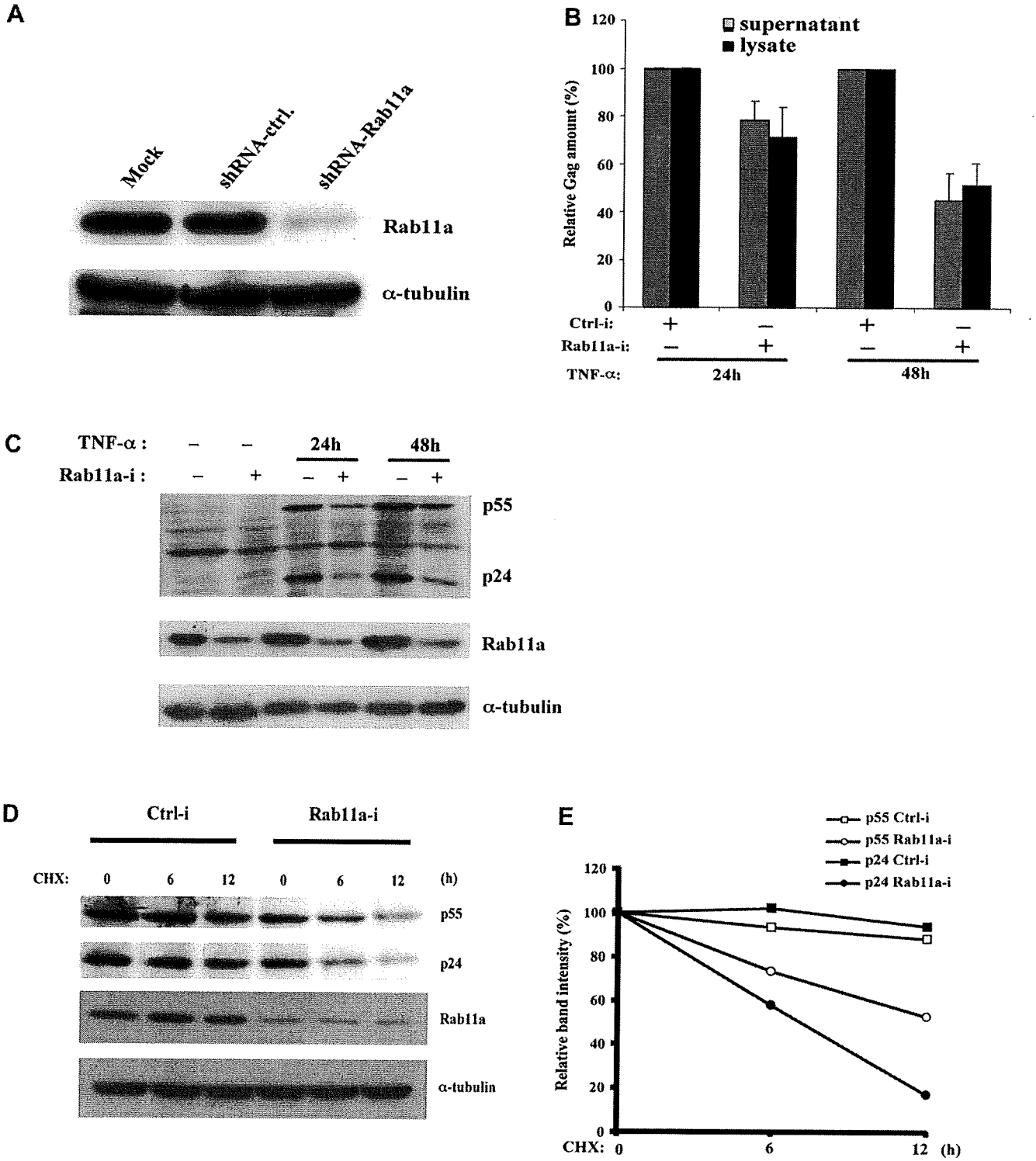

Fig. 5. Depletion of Rab11a destabilized HIV-1 Gag in U1 cells. (A) Whole-cell lysates (30 μg) prepared from U1 cells expressing control (Ctrl-i) or *rab11a*-specific (Rab11a-i) shRNA were subjected to 12% SDS–PAGE and immunoblotting with anti-Rab11a and anti-α-tubulin antibodies. (B) U1 cells expressing Ctrl-i or Rab11a-i were stimulated with TNF-α (1 ng/ml) for 24 or 48 h. Gag in supernatants and cell lysates was quantified, and the relative amounts of Gag are shown in percentage of that for cells expressing Ctrl-i (arbitrarily set at 100%). (C) Whole-cell lysates (30 μg) were prepared 24 or 48 h after TNF-α stimulation, and subjected to immunoblotting with the HIV-1-infected patient's serum, anti-Rab11a or anti-α-tubulin antibodies. (D) U1 cells expressing Ctrl-i or Rab11a-i were stimulated with TNF-α (1 ng/ml) for 24 h. Cells were then treated with cycloheximide (50 μM) for the indicated periods of time and whole-cell lysates (30 μg) were subjected to immunoblotting with the HIV-1-infected patient's serum, anti-Rab11a or anti-α-tubulin antibodies. (E) The relative band intensities of Gag (p55 and p24) normalized by that of α-tubulin are shown in percentage of that of cells before the addition of cycloheximide (arbitrarily set at 100%).

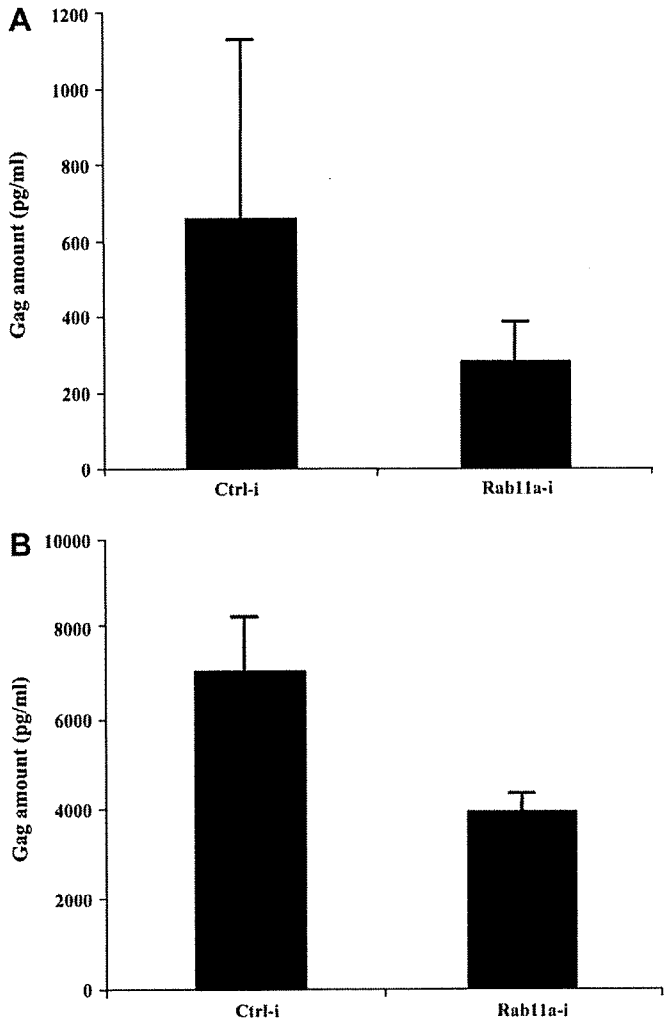

Fig. 6. Depletion of Rab11a reduced HIV-1 production in NOG mice. NOG mice (four mice in each group) were injected intraperitoneally with approximately 2.5×10^6 U1 cells expressing either Ctrl-i or Rab11a-i. The amounts of Gag in serum (A) and ascites (B) were quantified 2 weeks after cell inoculation.

be therapeutically more beneficial, because GGTIs do not work specifically on particular GTPases.

In summary, the present study revealed a critical role for protein geranylgeranylation in HIV-1 virion release from chronically HIV-1-infected promonocytic cells, and suggest that geranylgeranyltransferase-1 or its substrates, small GTPases involved in Gag trafficking, could be attractive molecular targets for controlling HIV-1 replication.

Acknowledgement

We thank Dr. Chen for the pHCMV-VSV-G and pCMVΔR8.2 plasmids. We also thank the members of Department of Molecular Virology, Tokyo Medical and Dental University for their advices and assistance with the experiments. This work was supported by grants from the Ministry of Education, Science and Culture; the Ministry of Health, Labor and Welfare; and Human Health Science of Japan.

References

[1] Y. Han, M. Wind-Rotolo, H.C. Yang, J.D. Siliciano, R.F. Siliciano, Experimental approaches to the study of HIV-1 latency, Nat. Rev. Microbiol. 5 (2007) 95–106.
[2] J.N. Blankson, D. Persaud, R. Siliciano, The challenge of viral reservoirs in HIV-1 infection, Annu. Rev. Med. 53 (2002) 557–593.
[3] T.W. Chun, R.T. Davey Jr., M. Ostrowski, J. Shawn Justemente, D. Engel, J.I. Mullins, A.S. Fauci, Relationship between pre-existing viral reservoirs and the re-emergence of plasma viremia after discontinuation of highly active anti-retroviral therapy, Nat. Med. 6 (2000) 757–761.
[4] G. del Real, S. Jimenez-Baranda, E. Mira, R.A. Lacalle, P. Lucas, C. Gomez-Mouton, M. Alegret, J.M. Pena, M. Rodriguez-Zapata, M. Alvarez-Mon, C. Martinez-A, S. Manes, Statins inhibit HIV-1 infection by down-regulating Rho activity, J. Exp. Med. 200 (2004) 541–547.
[5] C. Gilbert, M. Bergeron, S. Methot, J.F. Giguere, M.J. Tremblay, Statins could be used to control replication of some viruses, including HIV-1, Viral Immunol. 18 (2005) 474–489.
[6] J.F. Giguere, M.J. Tremblay, Statin compounds reduce human immunodeficiency virus type 1 replication by preventing the interaction between virion-associated host intercellular adhesion molecule 1 and its natural cell surface ligand LFA-1, J. Virol. 78 (2004) 12062–12065.
[7] G. Audoly, M.R. Popoff, P. Gluschankof, Involvement of a small GTP binding protein in HIV-1 release, Retrovirology 2 (2005) 48.
[8] A.A. Nabatov, G. Pollakis, T. Linnemann, W.A. Paxton, M.P. de Baar, Statins disrupt CCR5 and RANTES expression levels in CD4+ T lymphocytes in vitro and preferentially decrease infection of R5 versus X4 HIV-1, PLoS ONE 2 (2007) e470.
[9] T.M. Bocan, Pleiotropic effects of HMG-CoA reductase inhibitors, Curr. Opin. Investig. Drugs 3 (2002) 1312–1317.
[10] P.A. Konstantinopoulos, M.V. Karamouzis, A.G. Papavassiliou, Post-translational modifications and regulation of the RAS superfamily of GTPases as anticancer targets, Nat. Rev. Drug Discov. 6 (2007) 541–555.
[11] M.H. Gelb, L. Brunsveld, C.A. Hrycyna, S. Michaelis, F. Tamanoi, W.C. Van Voorhis, H. Waldmann, Therapeutic intervention based on protein prenylation and associated modifications, Nat. Chem. Biol. 2 (2006) 518–528.
[12] S.J. McTaggart, Isoprenylated proteins, Cell. Mol. Life Sci. 63 (2006) 255–267.
[13] B.L. Grosshans, D. Ortiz, P. Novick, Rabs and their effectors: achieving specificity in membrane traffic, Proc. Natl. Acad. Sci. U.S.A. 103 (2006) 11821–11827.
[14] S. Pfeffer, D. Aivazian, Targeting Rab GTPases to distinct membrane compartments, Nat. Rev. Mol. Cell Biol. 5 (2004) 886–896.
[15] G. Joberty, A. Tavitian, A. Zahraoui, Isoprenylation of Rab proteins possessing a C-terminal CaaX motif, FEBS Lett. 330 (1993) 323–328.
[16] J.L. Murray, M. Mavrakis, N.J. McDonald, M. Yilla, J. Sheng, W.J. Bellini, L. Zhao, J.M. Le Doux, M.W. Shaw, C.C. Luo, J. Lippincott-Schwartz, A. Sanchez, D.H. Rubin, T.W. Hodge, Rab9 GTPase is required for replication of human immunodeficiency virus type 1, filoviruses, and measles virus, J. Virol. 79 (2005) 11742–11751.
[17] O. Ullrich, S. Reinsch, S. Urbe, M. Zerial, R.G. Parton, Rab11 regulates recycling through the pericentriolar recycling endosome, J. Cell Biol. 135 (1996) 913–924.
[18] V. Varthakavi, R.M. Smith, K.L. Martin, A. Derdowski, L.A. Lapierre, J.R. Goldenring, P. Spearman, The pericentriolar recycling endosome plays a key role in Vpu-mediated enhancement of HIV-1 particle release, Traffic 7 (2006) 298–307.
[19] Y. Hamamoto, K. Takamatsu, S. Kobayashi, K. Yamaguchi, N. Yamamoto, N. Kobayashi, Characterization of human T-cell lines harboring defective human immunodeficiency virus type 1, Virus genes 3 (2) (1989) 141–152.
[20] M.Z. Dewan, K. Terashima, M. Taruishi, H. Hasegawa, M. Ito, Y. Tanaka, N. Mori, T. Sata, Y. Koyanagi, M. Maeda, Y. Kubuki, A. Okayama, M. Fujii, N. Yamamoto, Rapid tumor formation of human T-cell leukemia virus type 1-infected cell lines in novel NOD–SCID/

gammac(null) mice: suppression by an inhibitor against NF-kappaB, J. Virol. 77 (2003) 5286–5294.
[21] B.F. Fernie, G. Poli, A.S. Fauci, Alpha interferon suppresses virion but not soluble human immunodeficiency virus antigen production in chronically infected T-lymphocytic cells, J. Virol. 65 (1991) 3968–3971.
[22] T.M. Folks, J. Justement, A. Kinter, C.A. Dinarello, A.S. Fauci, Cytokine-induced expression of HIV-1 in a chronically infected promonocyte cell line, Science 238 (1987) 800–802.
[23] M. Perlmen, M.D. Resh, Identification of an intracellular trafficking and assembly pathway for HIV-1 gag, Traffic 7 (2006) 731–745.
[24] B. Grigorov, F. Arcanger, P. Roingeard, J.L. Darlix, D. Muriaux, Assembly of infectious HIV-1 in human epithelial and T-lymphoblastic cell lines, J. Mol. Biol. 359 (2006) 848–862.
[25] A. Ono, E.O. Freed, Cell-type-dependent targeting of human immunodeficiency virus type 1 assembly to the plasma membrane and the multivesicular body, J. Virol. 78 (2004) 1552–1563.
[26] A. Pelchen-Matthews, B. Kramer, M. Marsh, Infectious HIV-1 assembles in late endosomes in primary macrophages, J. Cell Biol. 162 (2003) 443–455.
[27] G. Raposo, M. Moore, D. Innes, R. Leijendekker, A. Leigh-Brown, P. Benaroch, H. Geuze, Human macrophages accumulate HIV-1 particles in MHC II compartments, Traffic 3 (2002) 718–729.
[28] M.D. Resh, Intracellular trafficking of HIV-1 Gag: how Gag interacts with cell membranes and makes viral particles, AIDS Rev. 7 (2005) 84–91.
[29] A. Savina, M. Vidal, M.I. Colombo, The exosome pathway in K562 cells is regulated by Rab11, J. Cell Sci. 115 (2002) 2505–2515.
[30] A. Vogt, J. Sun, Y. Qian, A.D. Hamilton, M. Saïd, The geranylgeranyl-transferase-I inhibitor GGTI-298 arrests human tumor cells in G0/G1 and induces p21 in a p53-independent manner, J. Biol. Chem. 272 (1997) 27224–27229.

AIDS RESEARCH AND HUMAN RETROVIRUSES
Volume 24, Number 3, 2008

DOI: 10.1089/aid.2007.0092

Enhancement of OX40-Induced Apoptosis by TNF Coactivation in OX40-Expressing T Cell Lines *in Vitro* Leading to Decreased Targets for HIV Type 1 Production

YOSHIAKI TAKAHASHI,[1,*] REIKO TANAKA,[1] NAOKI YAMAMOTO,[2] and YUETSU TANAKA[1]

ABSTRACT

OX40, a member of the tumor necrosis factor receptor (TNF-R) superfamily, has been shown to play an important role in the survival of antigen-specific CD4$^+$ T cells. We have previously reported that stimulation of the OX40-expressing and HIV-1 chronically infected T cell line, ACH-2/OX40, with either OX40 ligand (OX40L)-expressing cells or with TNF resulted in the activation of HIV-1 followed by apoptotic cell death. In the present study we found that costimulation via OX40 and TNF-R in OX40-expressing HIV-1-infected T cell lines leads to a marked reduction of HIV-1 production associated with rapid cell death. Since HIV-1-negative OX40$^+$ T cell lines underwent rapid apoptotic cell death after OX40L and TNF stimulation, it was reasoned that the ACH-2/OX40 cell death was unlikely to be due to HIV-1 infection. Furthermore, we found that the OX40-mediated apoptosis of the CD4$^+$ T cell line, Molt-4/CCR5-OX40 (M/R5-OX40), required (1) signals mediated via the cytoplasmic tail of OX40, (2) activation of the caspase cascade, including caspase-8 and caspase-3, and (3) induction of endogenous TNF-α, but not of TNF-β, FasL, or TNF-related apoptosis-inducing ligand (TRAIL), suggesting that this apoptosis occurred indirectly via the TNF/TNF-R system. Finally, a fraction of primary activated CD4$^+$ T cells, expressing high levels of OX40, underwent apoptosis, as revealed by annexin V staining, after cocultivation with OX40L$^+$ cells. These results suggest a new biological role of the OX40L/OX40 system in controlling the fate of activated CD4$^+$ T cells and of controlling HIV-1 infection in inflammatory environments.

INTRODUCTION

OX40 (CD134) is a 50-kDa transmembrane protein that serves as a marker of activated T cells. It is a member of the tumor necrosis factor receptor (TNF-R) superfamily, a family that also includes TNF-R1, TNF-R2, CD30, CD40, CD27, CD95 (Fas), TNF-related apoptosis-inducing ligand receptor (TRAIL-R) 1, and TRAIL-R2.[1–3] Its ligand, in humans, OX40L (CD252), was originally identified on human T cell leukemia virus type-1 (HTLV-I)-infected T cell lines and was termed gp34.[4,5] OX40L belongs to the tumor necrosis factor (TNF) superfamily[6] and is expressed predominantly on normal activated dendritic cells (DCs),[7] B cells,[8,9] vein endothelial cells,[10] and stimulated monocytes.[11] OX40-mediated costimulation of CD4$^+$ T cells by OX40L induces nuclear factor-kappa B (NF-κB) activation through TNF-R-associated factor (TRAF)2 and TRAF5,[12] and is associated with a number of immune function activities. These include the enhanced synthesis of T helper (Th) 2 responses from naive CD4$^+$ T cells,[13–15] the production of both Th1 and Th2 cytokines,[16–18] the development and survival of memory CD4$^+$ T cells,[17] the prevention of peripheral CD4$^+$ T cell tolerance,[19] and the ability to block the inhibitory activity of CD4$^+$ CD25$^+$ T regulatory cells.[20] Ligation of OX40L on activated B cells and on immature DC, *in vitro*, results in enhanced immunoglobulin production[9] and maturation of DC,[7] respectively. In addition to these costimulatory functions, additional OX40/OX40L functions include not only the promotion of cell-to-cell adhesion between activated or HTLV-I$^+$ leukemic CD4$^+$ T cells and OX40L$^+$ vein endothelial cells,[21] but also the migration of CD4$^+$ T cells to B cell follicles in pe-

[1]Department of Immunology, Graduate School of Medicine, University of the Ryukyus, Okinawa 903-0215, Japan.
[2]AIDS Research Center, National Institute of Infectious Diseases, Tokyo 162-8640, Japan.
*Present address: AIDS Research Center, National Institute of Infectious Diseases, Tokyo 162-8640, Japan.

ripheral lymph nodes.[22] The failure to properly control OX40/OX40L interaction has been suggested to cause immune abnormalities such as autoimmune diseases,[23–25] allergy,[26,27] or defective protection against pathogens.[15,28–30]

In addition to its ability to induce cell activation, the TNF-R superfamily is also associated with promoting cell death. One group of the TNF-R superfamily, consisting of Fas, TNF-R1, TRAIL-R1, and TRAIL-R2, mediates cell death through their intracytoplasmic death domain (DD). A second group, consisting of the DD-lacking receptors, TNF-R2, CD27, CD30, CD40, 4-1BB, and OX40, is capable of inducing cell death under certain conditions. Thus, for example, activation of TNF-R2 triggers apoptosis of a rhabdomyosarcoma cell line and of HeLa cells.[31] The activation of CD27 induces apoptosis of B cell lines[32] and the activation of CD30 by specific antibody mediates apoptosis of an anaplastic large cell lymphoma[33] and of a T cell hybridoma costimulated with anti-T cell receptor (TCR).[34] In addition, the activation of CD40 by antibody induces apoptosis in transformed cell lines and in normal activated $CD4^+$ T cells costimulated with anti-CD3 antibody.[31,35] The precise mechanisms of cell death induced by the DD-lacking TNF-R superfamily remain to be elucidated. Recently, it has been shown that TNF-R2 stimulation causes TNF-R1-dependent apoptosis by the depletion of the antiapoptotic proteins TRAF2 and IAP.[36,37] We have previously shown that OX40 stimulation activates human immunodeficiency virus type-1 (HIV-1) production in the chronically HIV-1-infected T cell line ACH-2/OX40 through the activation of NF-κB.[38] This mechanism is consistent with another member of the TNF-R superfamily, CD30.[39] Following stimulation with either OX40L or TNF, ACH-2/OX40 cells undergo not only HIV-1 activation but also apoptotic cell death within 48 h.[38]

In the present study, we examined the fate of cells following either OX40 stimulation alone or stimulation with OX40 in combination with TNF. Surprisingly, costimulation resulted in a marked decrease of HIV-1 production, as a consequence of rapid cell death of the T cell line. The cell death was reasoned not to be secondary to HIV-1 infection since OX40 stimulation alone and/or costimulation with TNF also induced cell death of HIV-1-negative T cell lines. Furthermore, the cell death in the T cell lines via OX40 stimulation was mediated indirectly by the TNF/TNF-R system. These observations suggest a new immunological role of OX40.

MATERIALS AND METHODS

Reagents

The medium used consisted of RPMI 1640 medium (Sigma, St. Louis, MO), supplemented with 10% fetal calf serum (FCS; Sigma), 100 U/ml of penicillin, and 100 μg/ml of streptomycin (hereinafter called RPMI medium). Antihuman (h) CD3 (clone OKT-3) and anti-hCD4 (clone OKT-4) monoclonal antibodies (mAbs) were purchased from the American Type Culture Collection (Rockville, MD). Anti-hOX40 mAb (clone B-17D8; mouse IgG2b, κ) was newly generated by a previously described method.[38] Anti-hTNF-α, anti-hTNF-β, and anti-hTRAIL mAbs, for neutralization, were purchased from R&D (Minneapolis, MN). Anti-hFasL neutralizing mAb was purchased from BD Pharmingen (San Diego, CA). Anti-hCaspase-8 and anti-hCaspase-3 mAbs were purchased from Cell Signaling (Danvers, MA) and horseradish peroxidase (HRPO)-conjugated goat antimouse immunoglobulin G (IgG) Ab was purchased from Chemicon (Temecula, CA). Anti-hOX40L neutralizing mAb (clone 5A8)[40] and isotype control mouse IgG1 (mIgG1), anti-HTLV-I Tax mAb (clone TAXY-8),[41] have been described previously. Isotype control mIgG2a and mIgG2b were purchased from BD Pharmingen and ImmunoTools (Friesoythe, Germany), respectively. Recombinant human TNF-α (rhTNF-α), TNF-α (rhTNF-β), interleukin-4 (rhIL-4), and rhIL-12 were purchased from Peprotec (London, UK). rhIL-2 was purchased from Shionogi Pharmaceutical (Osaka, Japan). The broad-spectrum caspase inhibitor, z-VAD-fmk, was purchased from MBL (Nagoya, Japan), dissolved in dimethyl sulfoxide and diluted in medium prior to use. Apoptosis was assessed by the annexin V-fluorescein isothiocyanate (FITC)/propidium iodide (PI) staining kit (Sigma and R&D). The hTNF-α sandwich enzyme-linked immunosorbent assay (ELISA) kit was purchased from R&D. The advanced protein assay reagent was purchased from Cytoskeleton (Denver, CO).

Cells

The hOX40-transfected and the HIV-1 chronically infected human T cell line cells, ACH-2/OX40 (cell groups 4 and 10), and its vector control, ACH-2/control (mock), and the hOX40L-tranfected mouse SV-T2 cell line, SV-T2/OX40L (gp34), and its vector control, SV-T2/control (mock), have been previously described.[38] The cell lines utilized for transfections of OX40, OX40L, and control vector were the human T cell lines Molt-4/CCR5[42] [Molt-4/CCR5-OX40 (M/R5-OX40), -OX40L, and -control], CEM (CEM/OX40, /OX40L, and /control), Jurkat (Jurkat/OX40, /OX40L, and /control), and HIV-1 productively infected human T cell line Molt-4/IIIB [Molt-4/IIIB-OX40 (M/IIIB-OX40), -OX40L, and -control], the human promonocytic cell lines U937 (U937/OX40, /OX40L, and /control), THP-1 (THP-1/OX40, /OX40L, and /control), and HIV-1 chronically infected human promonocytic cell line U1 (U1/OX40, /OX40L, and /control), and the human B cell line BJAB (BJAB/OX40, /OX40L, and /control). Aliquots of each of these cell lines were transfected by electroporation of 10–15 μg of the individual plasmids, pCAGIPuro/OX40, pCAGIPuro/OX40L, and control pCAGIPuro, as previously described.[38] In addition, the Molt-4/CCR5 cell line was also transfected with an expression vector containing the OX40 cytoplasmic tail-deleted mutant, pCAGIPuro/OX40-del(6-725), constructed as previously described,[38] to generate Molt-4/CCR5-OX40del cells. For the selection of transfectants, 1 μg/ml puromycin (Wako, Osaka, Japan) was added to the culture media. Expression of OX40 or OX40L in selectively grown cells was determined by flow cytometric analysis, as previously described.[38]

Detection of cell death and apoptosis

SV-T2/OX40L and SV-T2/control stimulator cells were fixed with 4% paraformaldehyde (PFA) for 15 min and washed three times in phosphate-buffered saline (PBS) prior to use. The OX40-expressing responder cells, at 4×10^5 cells/ml, were cocultured with various ratios of PFA-fixed stimulator cells in RPMI medium in the presence or absence of rhTNF-α (2 ng/ml)

or in the presence or absence of rhTNF-β (10 ng/ml) in 48-well culture plates (0.5 ml/well). The cocultures were incubated overnight, or for the indicated periods, at 37°C in 5% CO_2 humidified atmosphere. For blocking of the OX40–OX40L interaction, anti-hOX40L mAb (5A8) was added at a final concentration of 10–40 μg/ml at 37°C for 1 h prior to coculture. In some cases, anti-hTNF-α, anti-hTNF-β, anti-hTRAIL, and anti-hFasL blocking mAbs were added at a final concentration of 30–100 μg/ml at 37°C for 1 h prior to coculture. For inhibition of the caspase-dependent pathways of apoptosis, z-VAD-fmk was included in the culture medium at concentrations of 100 μM. The viability of the responder cells was determined, in triplicate, using a hemocytometer after staining with 0.1% eosin-Y (Wako, Osaka, Japan). The eosin-Y-stained PFA-fixed stimulator SV-T2/OX40L or SV-T2/control cells could be easily distinguished from dead responder cells by their distinct morphology. Apoptotic and necrotic cells were detected by staining with annexin V-FITC and PI, according to the manufacturer's instructions, utilizing a FACSCalibur (Becton Dickinson, San Jose, CA). The data obtained were analyzed using CellQuest software (Becton Dickinson).

HIV-1 production assay

Production of HIV-1 was determined by the measurement of HIV-1 core p24 levels using a commercial ELISA kit (ZeptoMetrix Corporation, Buffalo, NY). Data were analyzed by the Student's *t*-test. To examine the effect of OX40L and/or TNF stimulation on HIV-1 acutely infected T cell lines, M/R5-OX40 and M/R5-control were infected with the HIV-1 molecular clone NL4-3[43] at a multiplicity of infection (MOI) of 0.01 in 0.1 ml for 3 h at 37°C, as previously described.[44] The infected cells were subsequently washed twice and cultured at 2×10^5 cells/ml for 24 h in 48-well culture plates (0.5 ml/well). The infected cells were cocultured with PFA-fixed SV-T2/OX40L or with PFA-fixed SV-T2/control cells at a cell-to-cell ratio of 2:1 in the presence or in the absence of rhTNF-α (2 ng/ml), for an additional 3 days. Cell-free supernatant fluid was collected and the levels of p24 were quantified.

Western blotting

Western blot analysis was performed as previously described.[38] Briefly, M/R5-OX40 cells (4×10^5 cells/well) were stimulated by PFA-fixed SV-T2/OX40L or by PFA-fixed SV-T2/control cells (2×10^5 cells/well) for 6 h in 12-well plates. Cell lysates were obtained by lysis of $2.5–4 \times 10^7$ cells in 1 ml of a lysis buffer (10 mM Tris–HCl, pH 8.0, 140 mM NaCl, 3 mM $MgCl_2$, 2 mM phenylmethylsulfonyl fluoride, 0.5% Nonidet P-40) on ice for 20 min, followed by centrifugation at $13,000 \times g$ for 10 min at 4°C. The cell lysates (6 μg protein/lane) were treated with an equal volume of 2× sample buffer [125 mM Tris–HCl, pH 6.8, 4% sodium dodecyl sulfate (SDS), 20% glycerol, 0.1% bromophenol blue] without 2-mercaptoethanol, separated by SDS–polyacrylamide gel electrophoresis (PAGE), using a 12.5% gel, and then transferred to Immobilon-P Transfer Membrane (Millipore, Bedford, MA). The membrane was blocked with a blocking buffer [1% bovine serum albumin (BSA) in PBS] at 4°C overnight and incubated with the primary anti-hCaspase-8 and anti-hCaspase-3 mAbs (1:1000) according to the manufacturer's instructions. Mem-

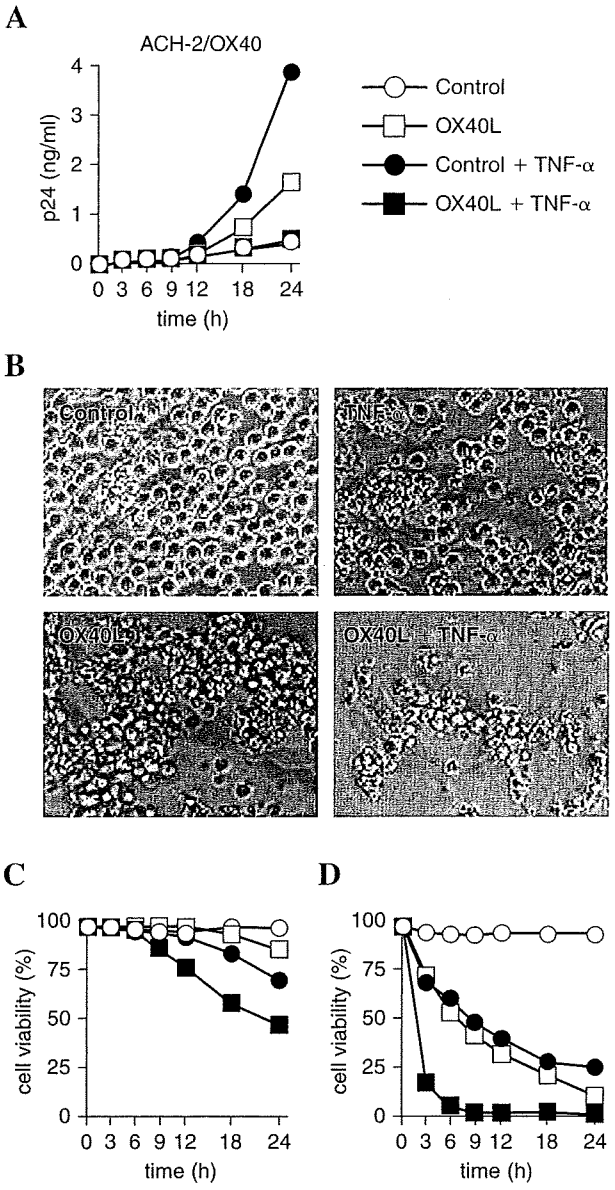

FIG. 1. Marked reduction of HIV-1 production and induction of rapid apoptosis by dual stimulation of ACH-2/OX40 cells with OX40L and TNF. ACH-2/OX40 cells (cell group 10) were cocultured with PFA-fixed SV-T2/OX40L (OX40L) or with PFA-fixed SV-T2/control (Control) cells in the presence or in the absence of TNF-α at 2 ng/ml for 24 h. (**A**) The kinetics of HIV-1 production, as determined by the level of HIV-1 p24 in the culture supernatants, (**B**) microscopic observation of morphological changes, (**C**) the kinetics of cell death as determined by an eosin-Y dye exclusion assay, and (**D**) the kinetics of apoptosis as determined by annexin V/PI staining. Morphological changes were examined under an inverted microscope at 100× original magnification. The cell viability was shown as percentage of control. Representative results from three independent experiments are shown. The data presented are the mean values ± SD of triplicate determinations.

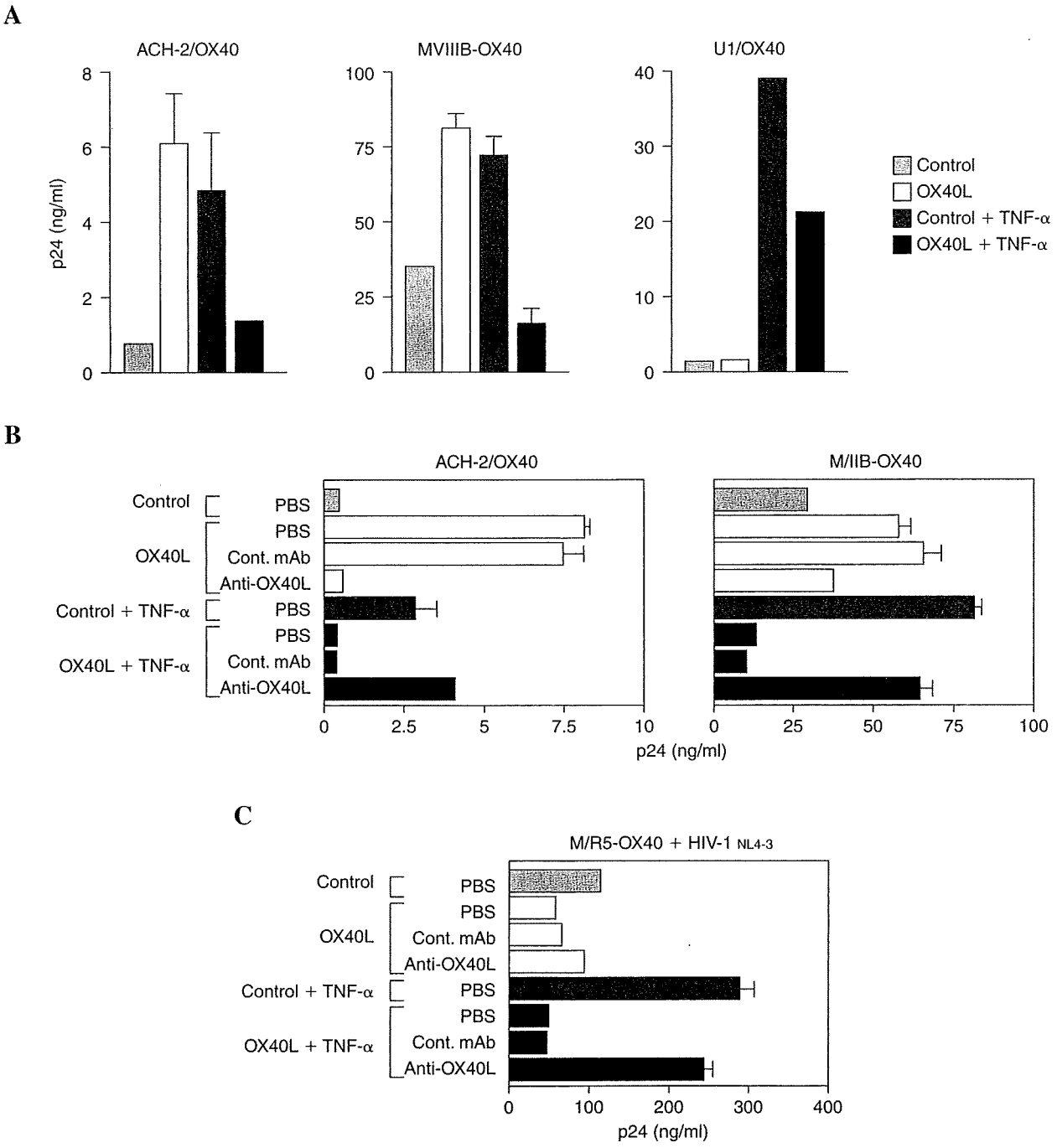

FIG. 2. Reduction of HIV-1 production in various HIV-1-infected cell lines. Several OX40-expressing cell lines were cocultured with PFA-fixed SV-T2/OX40L (OX40L) or with PFA-fixed SV-T2/control (Control) cells in the presence or absence of TNF-α (2 ng/ml) for 24 h. The levels of HIV-1 p24 produced in the culture supernatants were determined by ELISA. (**A**) Representative data was obtained using the HIV-1 chronically infected ACH-2/OX40 cells (cell group 4), the HIV-1 productively infected Molt-4/IIIB-OX40 cells (M/IIIB-OX40), and the HIV-1 chronically infected U1/OX40 cells. (**B**) The blocking effect of the anti-OX40L mAb (Anti-OX40L, 10 μg/ml for ACH-2/OX40 and 40 μg/ml for M/IIIB-OX40), negative control mAb (Cont. mAb, the same conditions as above) or of PBS was determined using ACH-2/OX40 and M/IIIB-OX40 cells. (**C**) The Molt-4/CCR5-OX40 cells (M/R5-OX40) were acutely infected with HIV-1_{NL4-3} at an MOI of 0.01, were precultured for 24 h, and were stimulated with OX40L and/or with TNF for an additional 72 h. The blocking effect of equal volumes of anti-OX40L mAb (Anti-OX40L, 10 μg/ml), negative control mAb (Cont. mAb, 10 μg/ml), or of PBS was determined. The data presented are the mean values ± SD of triplicate determinations. Representative results from three independent experiments are shown.

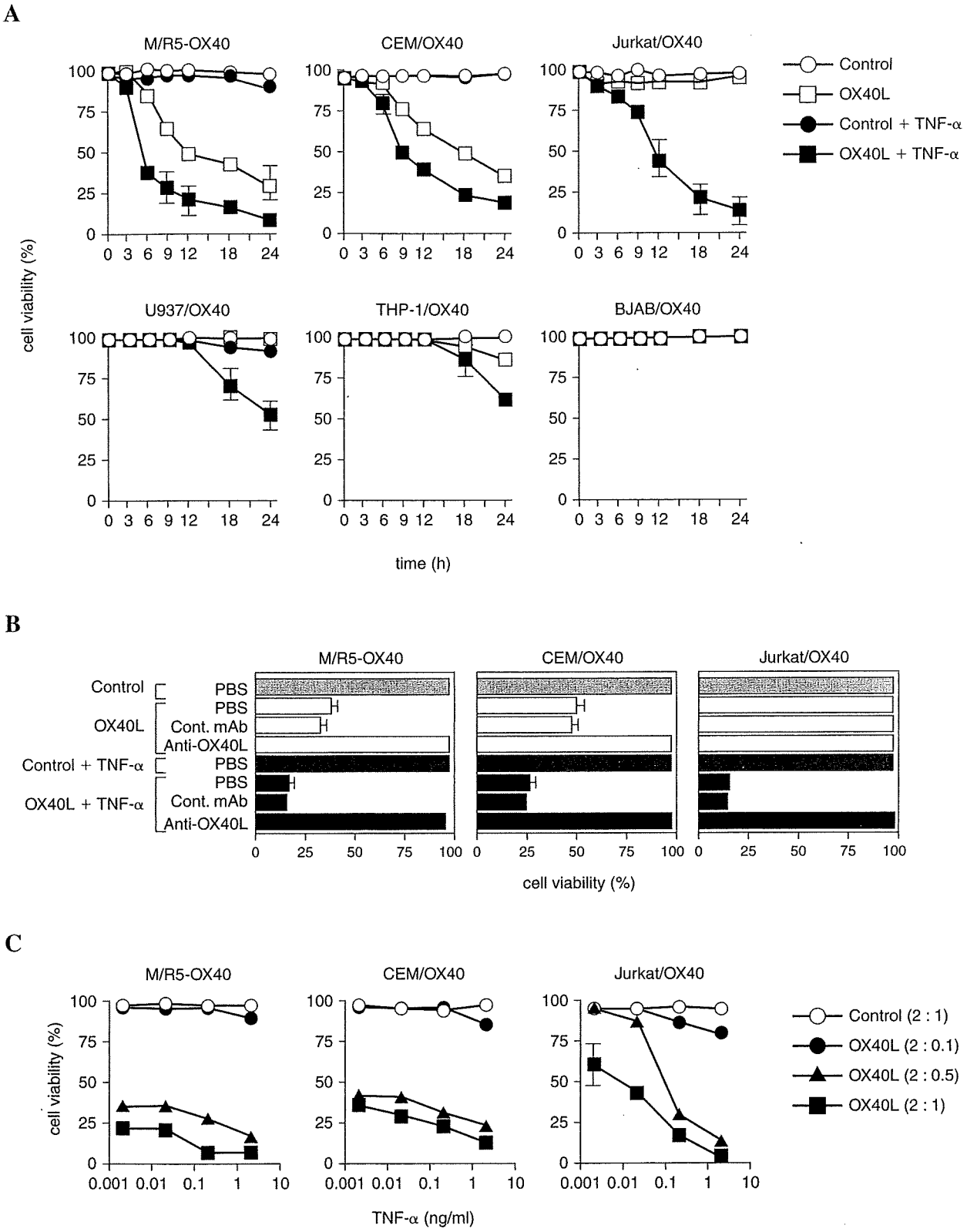

FIG. 3. Cell type-dependent induction of cell death by stimulation with OX40L alone or by combined activation with OX40L and TNF. Cell viability was determined by an eosin-Y dye exclusion assay, 24 h after stimulation by coculture with PFA-fixed SV-T2/OX40L (OX40L) or with PFA-fixed SV-T2/control (Control) cells in the presence or absence of TNF-α (2 ng/ml or graded concentrations). (**A**) The three CD4$^+$ T cell lines, Molt-4/CCR5-OX40 (M/R5-OX40), CEM/OX40, and Jurkat/OX40, the two promonocytic cell lines U937/OX40 and THP-1/OX40, and the B cell lines BJAB/OX40 were examined. (**B**) The blocking effect of anti-hOX40L mAb (Anti-OX40L, 10 μg/ml) on cell death of OX40-expressing CD4$^+$ T cell lines was determined. (**C**) The cell death of OX40-expressing CD4$^+$ T cell lines was induced by the addition of various concentrations of TNF-α, up to 2 ng/ml, and by various ratios of stimulator to responder cell. Data presented are the mean values ± SD of triplicate determinations. Representative results from three independent experiments are shown.

A

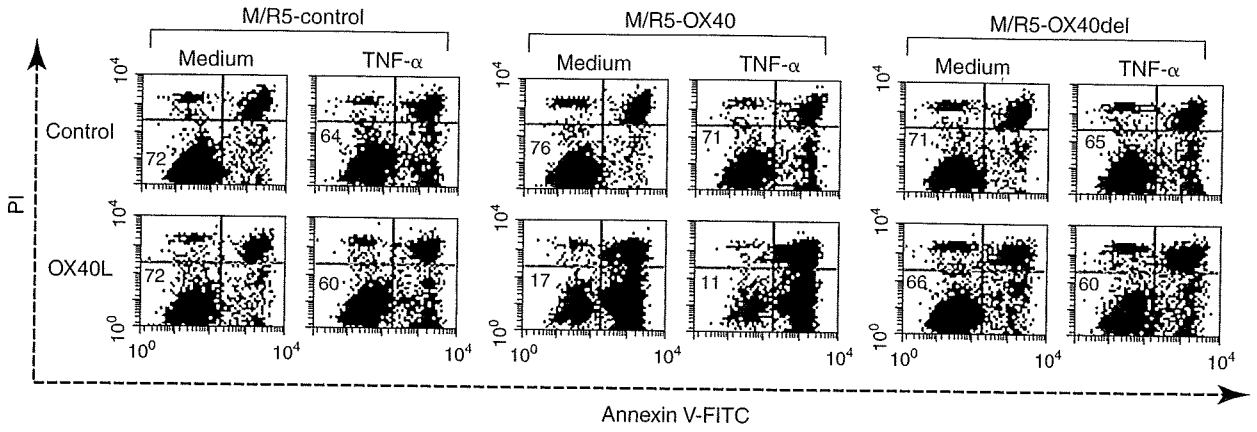
M/R5-control
M/R5-OX40
M/R5-OX40del
Medium
TNF-α
Control
OX40L
PI
Annexin V-FITC
72
64
76
71
71
65
72
60
17
11
66
60

B

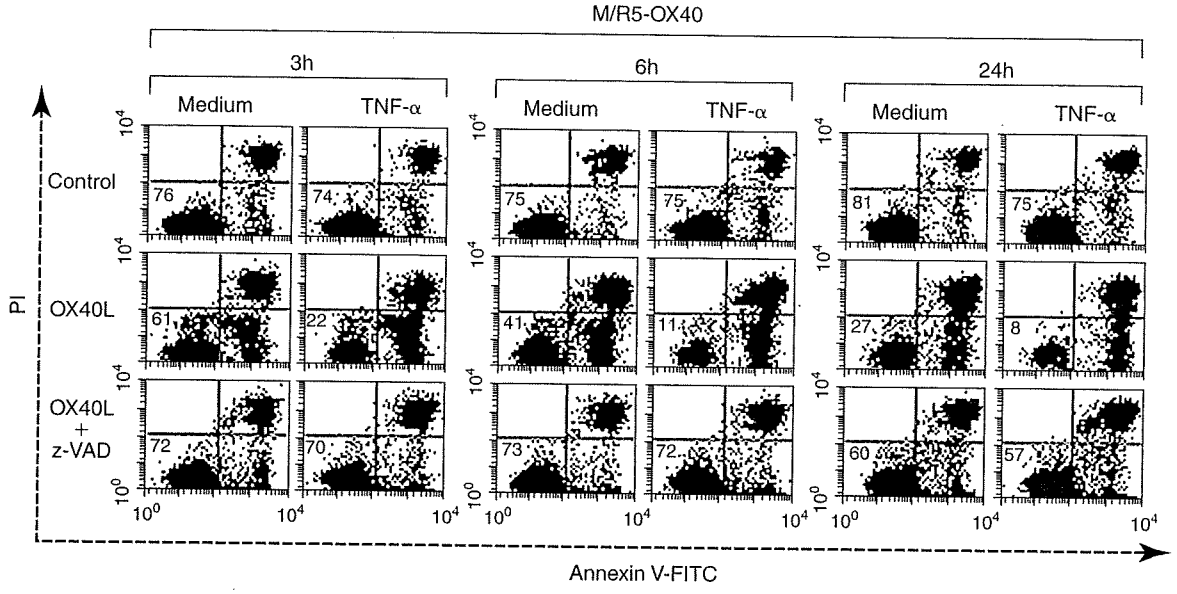
M/R5-OX40
3h
6h
24h
Medium
TNF-α
Control
OX40L
OX40L + z-VAD
PI
Annexin V-FITC
76
74
75
75
81
75
61
22
41
11
27
8
72
70
73
72
60
57

C

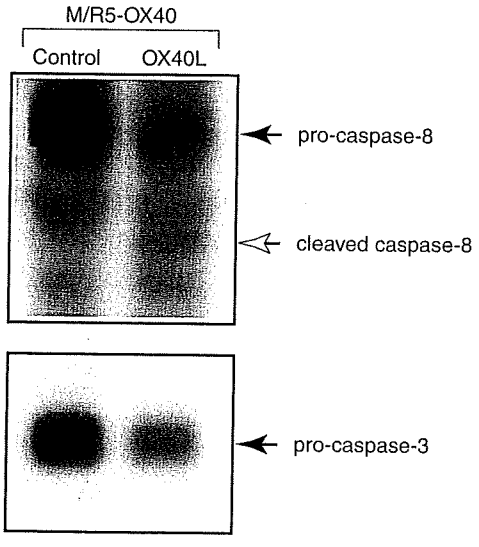
M/R5-OX40
Control
OX40L
pro-caspase-8
cleaved caspase-8
pro-caspase-3